Academic year 2011-2012

Technical Assessment and Modeling of Lithium-Ion Batteries for Electric Vehicles

Full Name of Student: *Dimitri Ottaviano*

Core Provider: *Carl von Ossietzky Universität Oldenburg - Ammerländer Heerstraße 114-118, 26129 Oldenburg, Germany*

Specialization: *Universität Kassel - Mönchebergstraße 19, 34109 Kassel, Germany*

Host Organization: *ETH Zurich - Paul Scherrer Institut Villigen, Switzerland*

Academic Supervisor: *Prof. Dr. Carsten Agert, NEXT Energy Oldenburg*

Specialist Supervisor: *Prof. Dr. Martin Braun, Fraunhofer IWES Kassel*

On – site supervisor: *Prof. Dr. Göran Andersson and Marina González Vayá, ETH Zurich*
Johannes Hofer, PSI Villigen

Submission Date: *3/12/2012*

Preface

This thesis is the last step of a path taken in May 2011, nineteen months ago, when I decided to apply for the EUREC European Master in Renewable Energy. This path has led me to live in two different countries working with people from all over the world and with completely different cultures and backgrounds but, above all, gave me the chance to get to know Friends who will remain part of my life forever. Friends with whom I spent a wonderful time and with whom I shared the joys and sorrows of this fantastic adventure.
This exciting and challenging journey started at Oldenburg, Germany, where I spent the core semester with the PPRE group of the Oldenburg University. Starting in 1987, the Postgraduate Program in Renewable Energy, is probably the oldest European Master related with RE. The core semester provided me with a sound understanding of the role of renewable energies in the energy sector together with a basic technical knowledge of the different renewable energy technologies.
The choice to specialize in Hybrid Systems took me to Kassel, where I attended the specialization semester. The main topic of the specialization is energy supply systems without connection to an electricity grid for application in rural areas like mountainous regions and locations in developing countries. The proximity and the close working relationships with Fraunhofer IWES and SMA, make the University of Kassel a centre of excellence in on- and off-grid systems research.
Upon completion of the specialisation, I moved to Zürich, Switzerland as a visiting student of ETH, the Swiss Federal Institute of Technology. The Eidgenössische Technische Hochschule Zürich is consistently ranked by all major World University rankings among the top universities in the world. Twenty-one Nobel Prizes have been awarded to students or professors of the Institute in the past, the most famous of which is Albert Einstein in 1921, and the most recent is Richard F. Heck, in 2010. In order to write my thesis, I did an internship at the Paul Scherrer Institut. At PSI, the largest research centre for natural and engineering sciences in Switzerland, I worked on the evaluation of Lithium-Ion batteries for EV and PHEV. My role as a MSc. student was aimed in particular at the assessment of Lithium-Ion battery performance taking into consideration various driving and weather conditions with the use of modeling tools that are calibrated for experimental measurements. The research was carried out within the THELMA project, a project aimed at understanding the multi-criteria, sustainability implications of widespread electric vehicles use in Switzerland. The project is being undertaken by a partnership of six different research groups within the domain of the ETHZ.

It would not have been possible to write this thesis and to pursue this degree without the help and support of the kind people around me. First of all I would like to thank my girlfriend, my family and friends for continuous support.
I would also like to thank Johannes Hofer and the LEA group at PSI together with Prof. Dr. Andersson and Marina González Vayá at ETH for their guidance during my internship.
Many thanks to my academic supervisor, Prof. Dr. Agert, to Dr. Blum, Edu, Hans, Udo and the PPRE staff at Oldenburg University. Your inputs for a greener world will not be in vain.
I would also like to thank Andre Bisévic for the passion he puts into his work and Prof. Dr. Martin Braun for the interest in my work.
“The Cat”, Pablito, μαλάκας, Aldo, Tunde, you know! I won’t say anything more!
Finally, special thanks go out to my special sponsor for its economic effort necessary to support me during these months.

Dimitri Ottaviano
Zurich, December 2012

Table of Contents

List of Figures

List of Tables

List of Abbreviations

AESC	Automotive Energy Supply Corporation
ASI	Area Specific Impedance
BatPac	Battery Pack Performance and Cost model
BEV	Battery Electric Vehicle
CRIEPI	Central Research Institute of the Electric Power Industry
DOD	Depth of Discharge
ESD	Energy Storage Device
EV	Electric Vehicle
EREV	Extended Range Electric Vehicle
FHEV	Full Hybrid Electric Vehicle
FTP	Federal Test Procedure
G	Graphite
HEV	Hybrid Electric Vehicle
ICE	Internal Combustion Engine
$LiCoO_2$ or LCO	Lithium Cobalt Oxide
$LiFePO_4$ or LFP	Lithium Iron Phosphate
$LiMn_2O_4$ or LMO	Lithium Manganese Oxide
$LiNiCoAlO_2$ or NCA	Lithium Nickel Cobalt Aluminum Oxide
$LiNiMnCoO_2$ or NMC	Lithium Nickel Manganese Cobalt Oxide
$Li_4Ti_5O_{12}$ or LTO	Lithium Titanate
MHEV	Mild Hybrid Electric Vehicle
NEDC	New European Driving Cycle
NiMH	Nickel Metal Hydride
NREL	National Renewable Energy Laboratory
OCV	Open Circuit Voltage
PHEV	Plug In Hybrid Electric Vehicle
P/E	Power to Energy Ratio
SEI	Solid Electrolyte Interface
SMES	Superconducting Magnetic Energy Storage
SOC	State of Charge
TEPCO	Tokyo Electric Power COmpany
USABC	United States Advanced Battery Consortium

Technical Assessment and Modeling of Lithium-Ion Batteries for Electric Vehicles

Dimitri Ottaviano, Carl von Ossietzky Universität Oldenburg, Germany

> *"As a country that has 2 percent of the world's oil reserves, but uses 20 percent of the world's oil — I'm going to repeat that — we've got 2 percent of the world oil reserves; we use 20 percent. What that means is, as much as we're doing to increase oil production, we're not going to be able to just drill our way out of the problem of high gas prices. Anybody who tells you otherwise either doesn't know what they're talking about or they aren't telling you the truth."*
> *President Obama, speech in North Carolina, March 7, 2012*

1. Introduction

1.1. Motivation

Coal has been the protagonist of the Industrial Revolution of the 18th and 19th century. With the advent of the automobile and aviation transport, oil became the dominant fuel during the twentieth century. In 2009 the world oil consumption was about 84.5 million barrels daily (about 88 in 2011), 35% of which was for land transport (BP, 2012), (IEA, 2012).
Some researchers argue that oil produced from conventional sources will be reduced by about 50% until 2030 (W. Zittel, 2007) with a consumption rate that continues unabated.
In addition to the limited fossil fuel resources, recent growing concern over the environmental impact of petroleum use has introduced the need to use alternative energy sources and electric vehicles.
Against this background, it is quite clear that modern society will be forced to face a drastic change in the way in which it produces and uses the available energy in the coming years.
Consequently, nowadays there is also an increased political pressure to produce and use "green" energy.
Although there are a number of possible solutions to the transportation challenge, such as the use of bio-fuels and hydrogen, many believe that hybridization and electrification of vehicles are best ways to address the issues that the transportation industry will face (D. Choi, 2011) and (Pesaran, 2010).
Batteries are one of the main challenges which the automotive industry has to meet in order to make a positive change.

Automotive companies have largely used NiMH batteries for hybrid vehicles in the last decade and these are still used today because of their low cost per Watt. However, limited SOC operation range and low energy density make them unsuitable for EVs (Broussely, 2010).
Electric vehicles should be able to provide high driving range, acceleration, and long life. They should also be able to accept high power chargers from regenerative braking and fast charging stations. These are challenges difficult to achieve for the majority of the existing energy storage devices.

The solution seems to come from Lithium-Ion battery technology. Lithium-Ion batteries have been widely used in portable applications, such as mobile phones and laptop computers. In recent years and at the moment they seem to be also the most promising technology for storing energy in electric and hybrid vehicles.

1.2. Aim of the Work and Thesis Outline

Electric vehicles have become an important policy option to reduce the dependence on fossil oil and mitigate climate change (M. Tran, 2012). Despite the enormous improvement in battery technology, such as Lithium-Ion chemistry, the most crucial component and at the same time the weakest link in the modern electrification of transportation is still the energy storage system (Pesaran, 2010).

One major uncertainty in evaluating the system “EV-Battery” is the dependence of battery efficiency, performance and lifetime on consumer usage (varying charging and discharging patterns) as well as the variation of operating conditions, such as temperature. The goal of this thesis is to assess these dependencies taking into consideration different Lithium-Ion battery types together with various driving, charging and ambient temperature conditions.
The main parameters of the different chemistries have been assessed at cell and pack level in order to have a general and easy method to compare the performance that each type of battery may have under typical EV operating conditions.

Within the term electric vehicles different vehicle configurations are considered and each of them has different characteristics. As a consequence, the specific battery properties vary considerably with the vehicle type considered. Furthermore, nowadays in the EV battery market a wide variety of different chemistries, cell designs, packaging, and possible battery pack configurations is present. Developing a battery system suitable for a certain application is not an easy task and different evaluations should be done. Pure electric vehicles should guarantee long electric driving range. To do so they need high-energy batteries, while the main characteristic of hybrid vehicles battery is power.

Battery energy and power are two main parameters to define battery performance and they are strongly affected by the internal resistance. The internal resistance, in turn, is influenced by the operating conditions (temperature, SOC, C-rate) and by the type of the Lithium-Ion battery. In the central part of this thesis its dependency from different temperature, SOC, and battery chemistries is analyzed.
In order to better understand the influence that these dependencies may have on battery performance, such as usable energy and power capability, cell simulation with different discharge and charge cycles is performed.

Finally the integration of the battery model into a vehicle model in order to assess how different charging/driving conditions may affect its efficiency is performed. Since the duration and efficiency of battery charging are becoming increasingly important parameters, particular emphasis is given on the analysis of the efficiency during fast charging conditions.

To the knowledge of the author there is no work in the literature, which evaluates the main parameters affecting battery performance - both on the cell and pack level - and studies its implications in terms of energy and power capability during driving and charging conditions.

This thesis is organized as follows.
Chapter 2 describes some basic battery concepts. In particular, the principle of operation of Lithium-Ion cells is explained and a general overview of different Lithium-ion chemistries presented.
Chapter 3 focuses on Lithium-Ion batteries design and its implications on performance. First a description of the different hybrid and electric vehicle technologies together with the requirements these vehicles have on the battery is given. Then a general overview of different design configuration of Lithium-Ion cells is shown, together with some current battery pack solutions. Calculations for estimating the internal resistance, weight, and cost of different Lithium-Ion chemistries are performed using an open source model developed at Argonne National Laboratory.
In Chapter 4 an analysis of the possible factors affecting the performance, efficiency and lifetime of Lithium-Ion batteries is performed.
Chapter 5, after a brief introduction on different types of battery models, introduces the model used for the simulation and shows the results on battery cells energy and power capability obtained at different discharging/charging rates and temperatures.
In Chapter 6 the batteries previously analyzed are integrated into an electric vehicle simulation model and, after a brief introduction of the model, battery efficiencies in different charging and driving conditions are evaluated.
Chapter 7 concludes this thesis.

2. Batteries: Basic Concepts and Definitions

This Chapter focuses on Lithium-Ion battery fundamentals. Some basic battery concepts and electrochemical principles of Lithium-Ion battery technology are explained followed by an overview of different Lithium-Ion battery types.

2.1 Basic Electrochemical Principles of Lithium-Ion Batteries

Batteries are *"electrochemical devices that convert chemical energy, contained in their active materials, into electrical energy by means of electrochemical oxidation-reduction reactions, which occur at the electrodes. In the case of a rechargeable system, the battery is recharged by a reversal of this process"* (Linden, 2002).

One or more cells are connected in series and in parallel, in order to provide the desired voltage and capacity, form the battery. The cell is the electrochemical unit that provides the electrical energy by direct conversion of the chemical energy stored in its active material through the oxidation and reduction reactions, which take place respectively at the anode and cathode (during discharging). In order to balance the flow of electrons (through an external circuit) from the anode to the cathode, an electrolyte is necessary. The electrolyte conducts the ions (from anode to cathode) maintaining the mass balance within the cell.

In Lithium-Ion batteries the cathode is made of a composite material that defines the type of the Lithium-Ion cell, while the anode is mainly made, with some exceptions, of graphite. The electrolyte may be liquid or made with polymeric materials.
In Figure 1 we can see the discharging and charging process of a Lithium-Ion cell. During the discharging phase the lithium ions diffuse from anode to cathode through the electrolyte and intercalate into the cathode. Electrons flow through an external circuit in the same direction. During the charging phase the reverse process will occur.

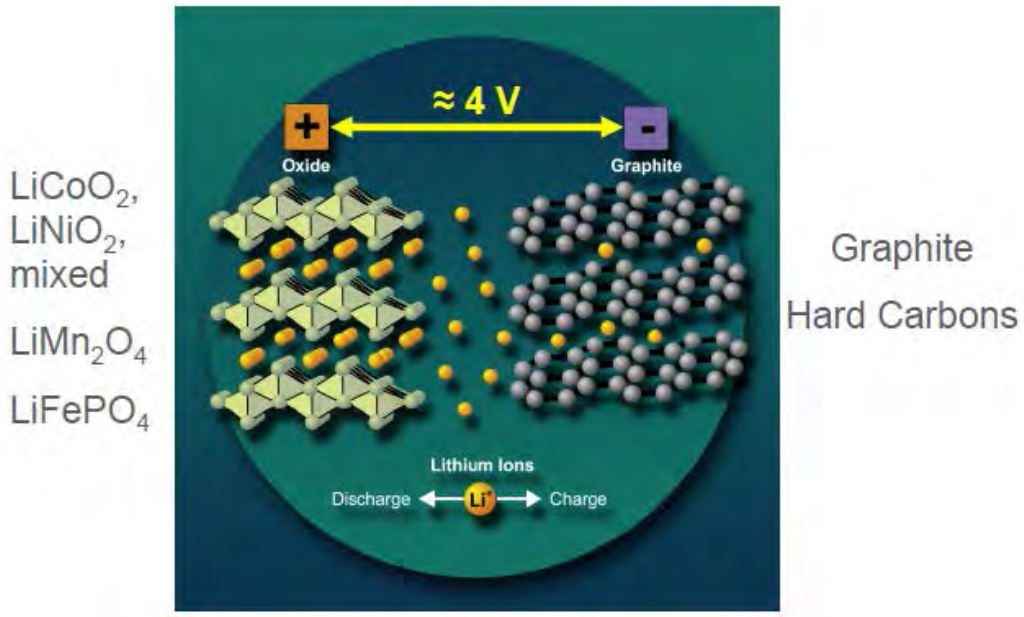

Figure 1: Discharging and charging process of Lithium-Ion cell (Novak)

2.2 Battery Definitions

In this section some basic definitions of the most important battery parameters used in this thesis are given.

2.2.1 Voltage and Capacity

The two most important parameters in a battery are the voltage and the capacity.
The *voltage*, expressed in Volt [V], measures the electrochemical potential available in the cell, which is determined by the type of active material contained in the cell.
The mass of the active material, however, determines the cell capacity. The *capacity* is a measure (in Ah) of the charge, which can be stored in the battery and gives an indication of the energy that can be extracted from the battery. The nominal rated capacity is usually defined by the battery manufacturers and determined under specific conditions. However, different operating conditions (i.e. high discharging/charging rates, temperature) and battery ageing can strongly affect the real capacity of the battery reducing the available stored energy.

2.2.2 SOC and DOC

The *State Of Charge (SOC)* of a battery can be defined as the proportion between the charge available at certain time and the total available charge when the battery is completely charged. It is in general expressed in percentage and varies between 0 and 100. In EV application, the SOC can be seen as the “fuel gauge” of the car, where the SOC indication replaces the fuel level indicator.
While the SOC can be seen as a measure of the capacity left in the battery, the *Depth Of Discharge (DOD)* indicates the charge removed from the battery and is expressed in percentage as well.

2.2.3 C-rate

Electric current is defined as a flow of electric charge. The SI unit of the electric current is the Ampere (A) but an alternative and maybe more intuitive measure of the current at which a battery is discharged (or charged) comes from the C-rate definition. The *C-rate* indicates the current needed to fully discharge (or charge) a battery in a determined period of time. For example a battery with a nominal capacity of 70 Ah can be fully charged in one hour applying a current of 70 A (C-rate=1) or in two hours at 35 A (C-rate=C/2), or in half an hour at 140 A (C-rate=2C).

2.2.4 Internal Resistance

Due to its extreme importance on battery performance, as we will see in the following chapters, most of the work done in this thesis focuses on the battery internal resistance.
The internal resistance of a battery cell depends on many factors (i.e. temperature, SOC and C-rate) and therefore, cannot be considered as a constant. It is generally used to model the voltage drop of the cell under load conditions and the associated power dissipation.
There are many different definitions of battery internal resistance present in the literature. The common property in these definitions is that the internal resistance acts in opposition to the current flow within the battery. Tahil (Tahil, 2010) and Guzzella (L. Guzzella A. S., 2007)

define the internal resistance as the sum of the ohmic, activation and diffusion polarization resistance, which is the largest possible voltage drop in the cell.

2.2.5 Energy and Power

The *Energy* of a battery is defined as the product between its capacity and its voltage:

$$E[Wh] = Capacity[Ah] \cdot Voltage[V]$$

Although the nominal energy depends on the intrinsic electrochemical characteristics of the cell (capacity and voltage mean quantity and type of material used), it is important to understand that the energy storage capabilities of a battery can vary significantly from their nominal values due to various factors such as ageing, temperature and operating conditions.

The battery terminal *Power* is defined as:

$$Power[W] = Voltage[V] \cdot Current[A]$$

The energy and power, together with cost, safety and lifetime, are the most important parameters to define battery performance. In this thesis however, cost, safety and lifetime, if not otherwise specified, will not be considered in the performance evaluation of the battery.
One common method to compare battery, and more in general energy storage devices, performance is the Ragone Plot (Figure 2). It provides the available specific energy (Y-axis) as a function of specific power (X-axis), or vice versa, in logarithmic axes. Christen and Carlen (T. Christen, 2000) characterized different Ragone curves for different types of energy storage device (ESD) highlighting the difference between inductive ESD (SMES or flywheels), where energy increase with power, and capacitive ESD (capacitor and batteries), where energy decreases with power. While batteries are the ESD with the highest available energy density (especially Lithium-Ion batteries), they are not yet able to completely fulfill the USABC (US Advanced Battery Consortium) requirements for EV applications (Srinivasan, 2008).

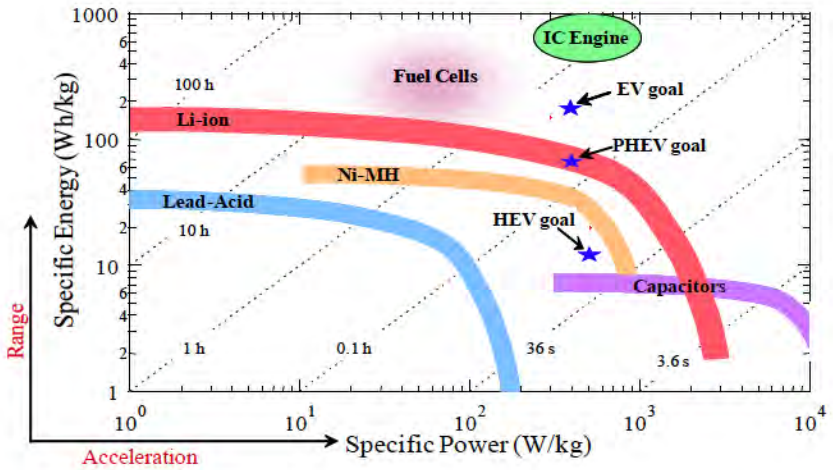

Figure 2: Ragone plot of various electrochemical energy storage and conversion devices. The USABC EV, PHEV and HEV battery requirements are shown as blue stars. For EV applications the specific energy can be seen as the vehicle range and specific power as the vehicle acceleration (Srinivasan, 2008)

2.3 Lithium-Ion Battery Types

The need of high energy density led to the fact that the most favored technology to store energy in EV and PHEV applications is the Lithium-Ion battery.
Many Lithium-Ion technologies are however available on the market nowadays and each of them has its own advantages and drawbacks (Figure 3). The different Lithium-Ion types are named according to the cathode and anode chemistry composition and are listed in Table 1.

Chemical Name	Material	Abbreviation	Notes
Lithium Cobalt Oxide	$LiCoO_2$	LCO (1)	High capacity. Used for cell phone and laptop
Lithium Manganese Oxide	$LiMn_2O_4$	LMO (1)	Most safe, lower capacity than LCO but high specific power and long life. Used for power tools, E-bikes, EV, medical.
Lithium Iron Phosphate	$LiFePO_4$	LFP (1)	
Lithium Nickel Manganese Cobalt Oxide	$LiNiMnCoO_2$	NMC (1)	
Lithium Nickel Cobalt Aluminium Oxide	$LiNiCoAlO_2$	NCA (1)	Gaining importance in electric powertrain and grid storage
Lithium Titanate	$Li_4Ti_5O_{12}$	LTO (2)	

Table 1: Various Lithium-Ion types (Battery University, 2012)
(1) Cathode material; (2) Anode material

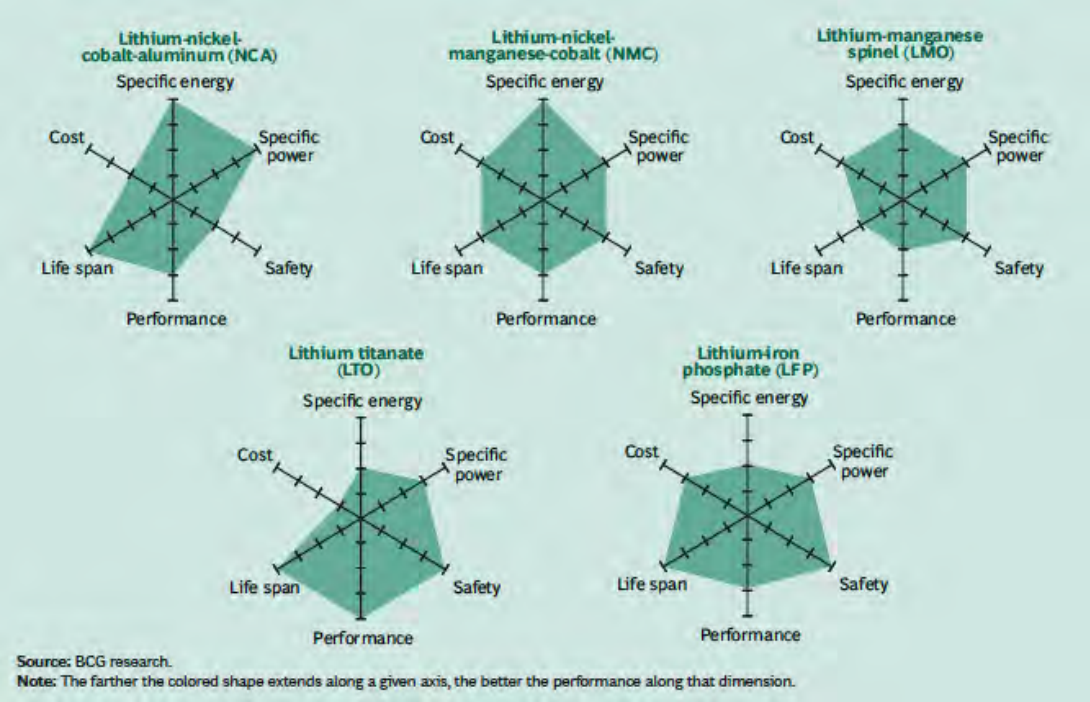

Figure 3: Comparison of various Lithium-Ion types (BCG, 2010)

3. Design and Performance of Lithium-Ion Batteries

This Chapter focuses on Lithium-Ion batteries design and performance. First a description of the different hybrid and electric vehicle technologies together with their required battery properties is given. Then a general overview of different design configurations of Lithium-Ion cells is shown. Moreover the description of some current battery pack solutions gives an insight into how the battery packs are made in the industry. Then the Battery Performance and Cost model (BatPac) developed at Argonne National Laboratory is explained. The BatPac is a model which can be used to compare the cost, mass, and power capability of various Lithium-Ion chemistries for different vehicle applications. In the last section of this chapter some of the results obtained using this model are discussed, showing the energy and power, internal resistance, weight and cost of a battery pack as a function of the battery chemistry.

3.1 Battery Requirements for Hybrid and Electric Vehicles

There are several different concepts covered by the terms hybrid and electric vehicles. This section presents a brief description of both the technologies followed by an analysis of requirements that batteries for hybrid and electric vehicles should comply with.

3.1.1 HEV Hybrid Electric Vehicles

Hybrid Vehicles can be classified as: Micro, Mild and Full Hybrid Electric Vehicles (Kohler, 2009).
Micro Hybrid Vehicles are a class of vehicles where the ICE is shut down automatically when the vehicle is stopped (start-stop system). This type of vehicle is able to achieve a reduction of fuel consumption in the range of 5 to 10% in urban driving conditions.
In a *Mild Hybrid Electric Vehicle (MHEV)* the battery system provides power and energy to the powertrain only during the start and acceleration phase. An important feature of this kind of vehicle is its ability to be regeneratively charged during deceleration and breaking. Their typical fuel consumption reduction ranges from 15 to 20%.
In *Full Hybrid Electric Vehicle (FHEV)* pure electric short driving range is provided. They can achieve a reduction of fuel consumption up to 40% thanks to an efficient combination of ICE and electrical driving system.

3.1.2 PHEV Plug In Hybrid Electric Vehicles and BEV Battery Electric Vehicles

A Plug-In Hybrid Electric Vehicle (PHEV) combines the advantages of a pure battery electric vehicle with those of an ICE vehicle. This class of vehicles is able to provide all electric range (up to 50 miles) thanks to a battery system that can be charged using power from the grid, just like a pure electric vehicle. Once the battery is discharged, the ICE is activated overcoming the limited range problem. This type of vehicles can drastically reduce, or even eliminate, the daily fuel consumption if the car is mainly used for short distances (i.e. home-office and return). The main drawback for this technology is the added cost and weight of the battery.
The *Battery Electric Vehicle (BEV)* is able to operate solely through the use of an electric motor entirely driven by the energy stored in a battery system. The battery can be recharged

connecting the vehicle to the grid. EVs are “zero local emissions” vehicles and in general they are much more efficient than ICE and hybrid vehicles with lower operating costs. The drawbacks are a limited driving range (low energy densities of current battery technologies) compared to fossil fuel, long charging time, lack of charging infrastructure, and high purchasing cost (Pesaran, 2010).

3.1.3 Battery Requirements for Hybrid and Electric Vehicles

As we have seen in the previous section, hybrid and electric vehicles have very different characteristics. As a consequence, the specific battery properties vary considerably with the vehicle type. Electric vehicles must guarantee long pure electric driving range and to do so they need high-energy batteries, whereas the main characteristic of the hybrid vehicles battery is the requirement to provide high power (Broussely, 2010). In Figure 4 and Table 2, the general power and energy ranges required for different types of electric and hybrid vehicles can be seen.

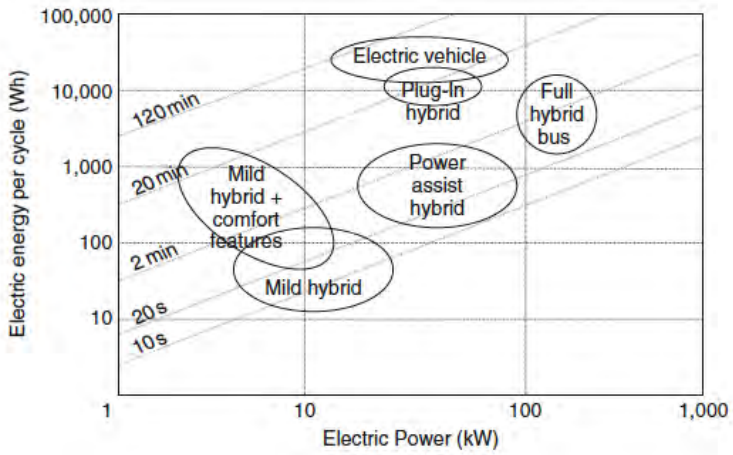

Figure 4: Power/Energy characteristics required from the battery by different types of electric and hybrid vehicles (Broussely, 2010)

EV type	Power range (kW)	Energy range (kWh)	Voltage range (V)
Micro-HEV	2.5–5	0.5	12–36
Mild HEV	15–20	1	120–160
Full HEV	30–50	2–3	200–350
FCHEV	25–30	1–2	220
Plug-in HEV	30–100 (Van)	5–15	200–350
EV	35–70 (Van)	25–40	200–350

Table 2: Different types of electric and hybrid vehicles and approximate Power/Energy requirements (Broussely, 2010)

The main requirement for Micro Hybrid batteries is the low cost. This type of batteries are frequently cycled in a short period of time and this aspect seriously compromises their lifetime making frequent battery replacements necessary ((Kohler, 2009) and (Broussely, 2010)).
MHEV and FHEV batteries must be able to accept high power peaks due to the regenerative breaking characteristics of this type of vehicles. In order to accomplish this requirement the most important characteristic that these batteries should have is a low internal resistance (Kohler, 2009). Moreover, they must be able to provide limited pure electric drive range. This requirement leads to the fact that the SOC has to be maintained at an intermediate level and

kept within certain limits ((Broussely, 2010) and (FCVT, 2007)). In Figure 5 we can see that these SOC range limits for PHEV are wider if compared to HEV. This is due to the fact that PHEV must guarantee a higher driving range in pure EV mode than normal HEV. An obvious consequence is a bigger battery size requirement.
As already mentioned, one of the most important technical property to be considered for pure EV batteries is the specific energy. Batteries for EV applications must provide a minimum pure electric range (high energy) and at the same time be suitable in terms of cost, dimension and weight. Other challenges are cycle and calendar life, and safety (Broussely, 2010). In order to be able to reduce charging time, as we will see later, particular attention has been given to fast charging. As a consequence, recently, the charging rate capability of these batteries has become another important requirement that must be fulfilled by EV batteries.

An important parameter which reflects the differences analyzed before is the P/E ratio shown in Figure 5. It can be defined as the peak power required for acceleration divided by the energy needed for range. The difference in P/E ratio is normally reflected as a difference in battery design since battery power is related to the electrodes surface area (high area, low resistance, high power) and energy is related to the type (voltage) and amount (capacity) of active material (FCVT, 2007).
Recycling and environmental issues are common requirements, which must be fulfilled by all the battery types and applications.

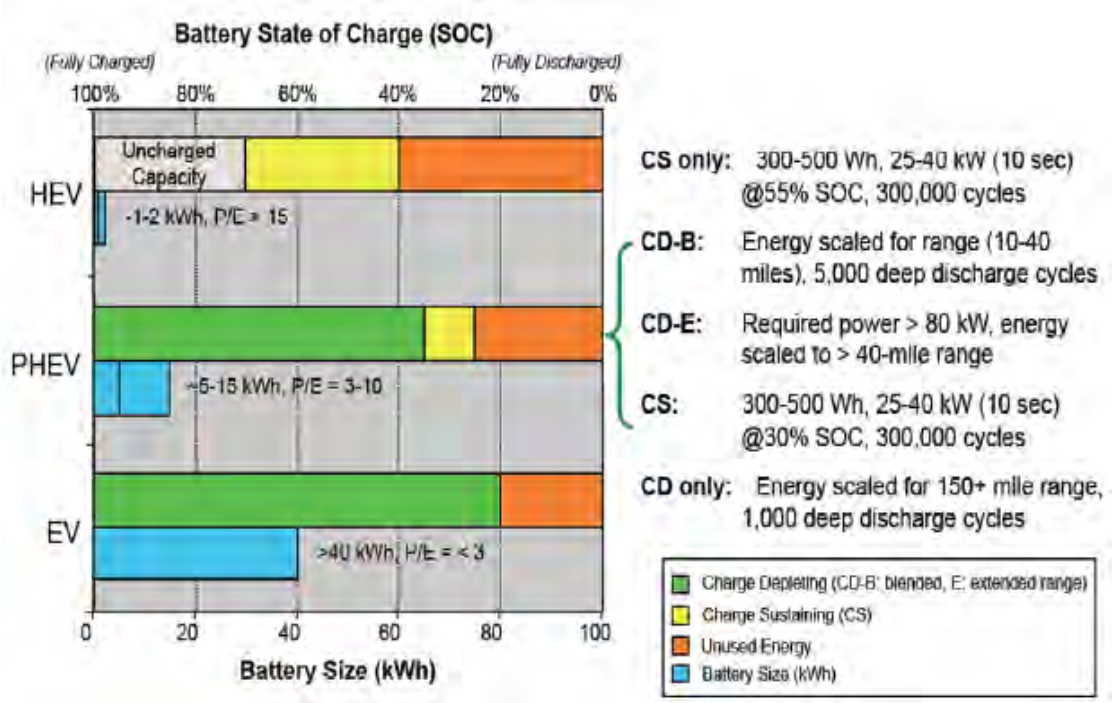

Figure 5: Battery performance requirements vs. vehicle application (FCVT, 2007)

3.2 Lithium-Ion Battery Design

Lithium-Ion battery designs vary with size and application and are in general available in four basic formats: cylindrical, coin, prismatic and pouch. However the general components used are the same. Figure 6 shows the four types of Lithium-Ion design.

With the exception of the Tesla Roadster, with a battery pack containing 6831 cylindrical cells (type 18650), battery packs for vehicle applications typically consist of a number of prismatic or pouch cells connected in series and/or in parallel.

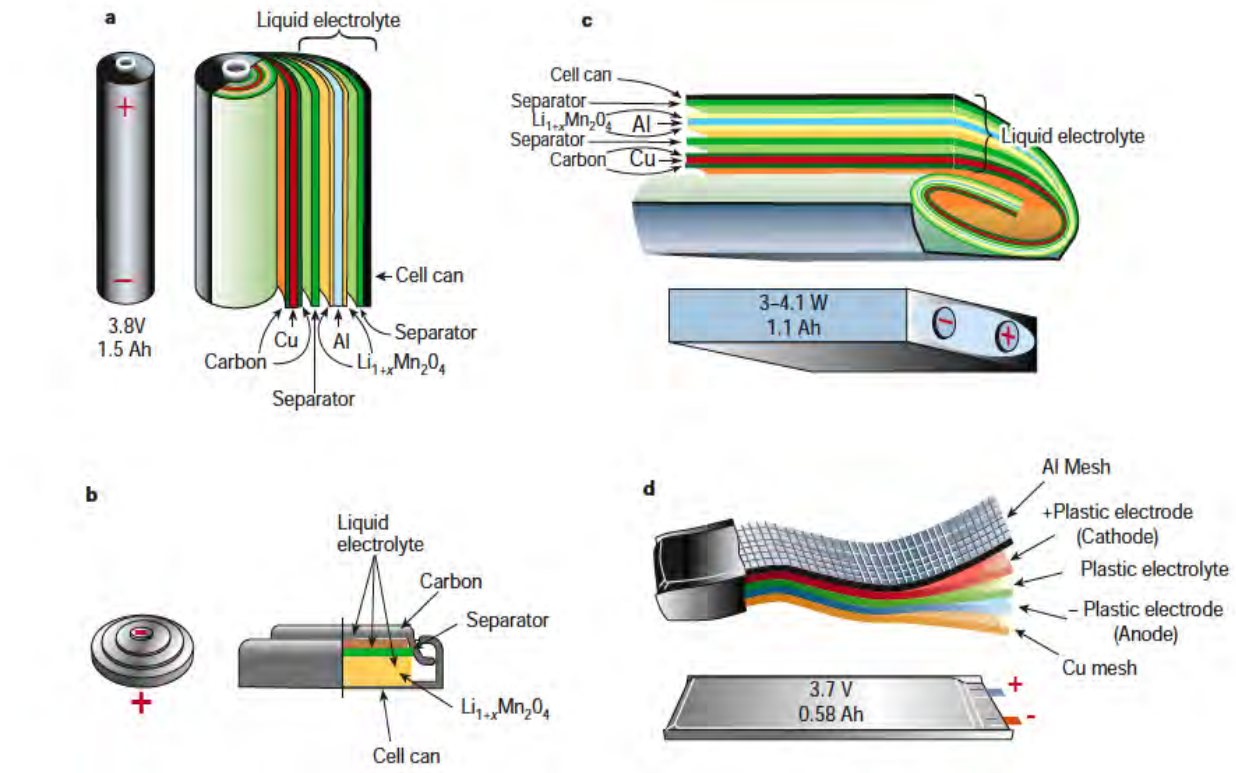

Figure 6: Different Lithium-Ion cell configurations: a) cylindrical, b) coin, c) prismatic, d) pouch (J.M. Tarascon, 2001)

3.3 Current Battery Pack Solution

In this section, an overview of the current battery pack solutions for some EVs and PHEVs present in the market today is provided. These configurations are further analyzed with the BatPac software presented in the following sections.

3.3.1 Chevrolet Volt

The Chevrolet Volt is a series PHEV. The battery drives the electric motor providing a full electric range for the first 25-50 miles. After that, once the battery is discharged, an internal gasoline generator provides electricity to the motor to extend the vehicle's range. This type of series configuration is usually termed EREV, Extended Range Electric Vehicle.
The Volt has a 16 kWh battery pack (45 Ah nominal capacity) containing 288 LG Chem's Lithium polymer cells (pouch design) with a manganese based cathode and carbon anode. The cells are arranged into three main modules that are positioned under the floor of the Volt structure. The entire Volt battery pack weighs around 180 kg (Abuelsamid, 2010).

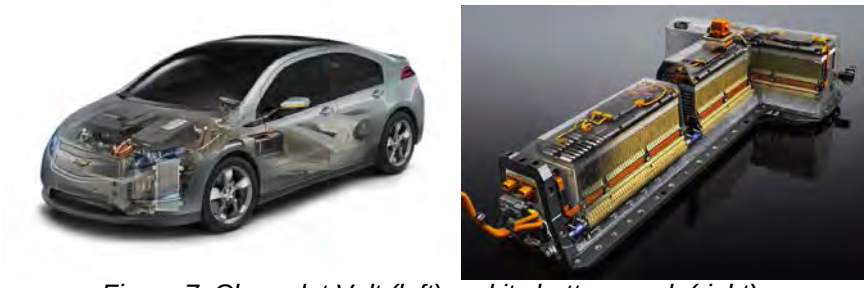

Figure 7: Chevrolet Volt (left) and its battery pack (right)

3.3.2 Nissan Leaf

The Nissan Leaf is a BEV that uses an 80 kW synchronous electric motor powered by a 24 kWh Lithium-Ion battery pack. The Leaf battery pack consists of 48 modules; each with four LMO-G cells (2 cells in series and 2 in parallel) for a total of 192 cells arranged in a big square and positioned under the car floor of the vehicle. The entire pack weighs around 270 kg (Blanco, 2010) and it is assembled by Automotive Energy Supply Corporation (AESC).

Figure 8: Nissan Leaf (left) and its battery pack (right) (Blanco, 2010)

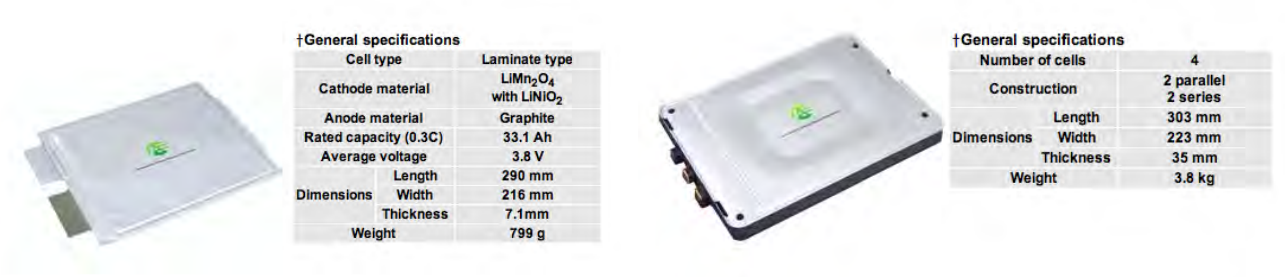

†General specifications

Cell type		Laminate type
Cathode material		$LiMn_2O_4$ with $LiNiO_2$
Anode material		Graphite
Rated capacity (0.3C)		33.1 Ah
Average voltage		3.8 V
Dimensions	Length	290 mm
	Width	216 mm
	Thickness	7.1mm
Weight		799 g

†General specifications

Number of cells		4
Construction		2 parallel 2 series
Dimensions	Length	303 mm
	Width	223 mm
	Thickness	35 mm
Weight		3.8 kg

Figure 9: Nissan Leaf cell (left) and module (right) specification (AESC, 2007)

3.4 Modeling of Battery Design and Performance

In this section some simulations using the BatPac model developed at Argonne National Laboratory are performed. The BatPac is a free source model useful to estimate costs and performances of different Lithium-Ion battery types for vehicle applications. The model allows the user to design a vehicle battery pack specifying the type of Lithium-Ion cell, the type of vehicle (BEV, PHEV or HEV) the battery pack configuration (number of cells in series and in parallel, number of modules, etc…), and the performance requirements (such as energy and

power). The model then calculates the physical properties of the battery based on the requirements defined and experimental data. Results are the dimensions, mass, volume, materials requirements, and cost for the cells, modules and battery pack (P.A. Nelson K. G., 2011). Another important parameter of the model is the Area Specific Impedance (ASI) of the cell. The battery internal resistance is calculated by taking into account the ASI of the electrode active material and the electrode area, as well as resistance occurring in electrical connections. The ASI depends on the Lithium-Ion chemistry as well as temperature and is fundamental in battery design, however, a detailed study of the ASI is not the scope of this work and therefore will not be treated in this thesis. Those interested in the derivation or further details can obtain more details in the following publications: (P.A. Nelson K. G., 2011) and (K.G. Gallagher, 2011).

Concerning the cost, the model calculates the annual materials cost, which is based on the material requirements of the battery pack configuration. The annual manufacturing cost is added to the materials cost and both are scaled from a baseline manufacturing plant with an annual production of 100.000 battery units. Additional expenses for operating the plant (i.e. administration, sales, depreciation of the initial investment) are further added and all costs are evaluated for 2020 when large EV battery manufacturing plants are supposed to be built.
Due to those and other assumptions, listed in (P.A. Nelson, 2011) and used in the BatPac model to simplify the cost calculation, the costs calculated and presented in the following have to be taken with caution and should be considered useful only as a rough estimation.

Using the BatPac model we have calculated the internal resistance, specific energy and power, together with other parameters such as specific battery cost (in $/kWh) and weight for different Lithium-Ion chemistries for current and next generation electric cars. For the calculation of the specific energy (both cell and pack values) we used the available energy, which is based on the SOC range used by the respective type of car and chemistry. For all the graphite-based chemistries, PHEV batteries utilize a portion of 70% of the total energy (cell thickness 6 mm), while EV batteries use 80% of their total energy (cell thickness 8 mm). Since the lithium titanate spinel anode has almost no risk of lithium plating on its surface, a higher percentage of cell capacity is available and the SOC range can be extended (M.Q. Synder, 2007). On this basis, the available energy for LMO-LTO battery is increased by 5% for both the vehicle type (75% of the total energy for PHEV and 85% for EV).
Because of their strong presence in the today's electric-drive market, we decided to use the Nissan Leaf configuration for the EV calculations and the Chevy Volt configuration for PHEV calculations. In order to have a good comparison between the various chemistries, the evaluation has to be done at a fixed battery pack voltage level. To do so, we had to change the battery pack configuration for the various types of Lithium-Ion batteries, adding more cells, or modules, in series until we reached the desired voltage level.
As mentioned above the calculated costs are only useful to get an idea for a possible comparison between the different Lithium-Ion battery types. Pesaran (Pesaran, 2010) provides a more reliable specific cost range for current high-energy batteries for EVs and PHEVs application, which is 500-800/kWh.
Figure 10 shows respectively the typical EV battery and cell parameters calculated for the different Lithium-Ion battery chemistries present in the BatPac model. Figure 11 shows the same results for a typical PHEV battery configuration.

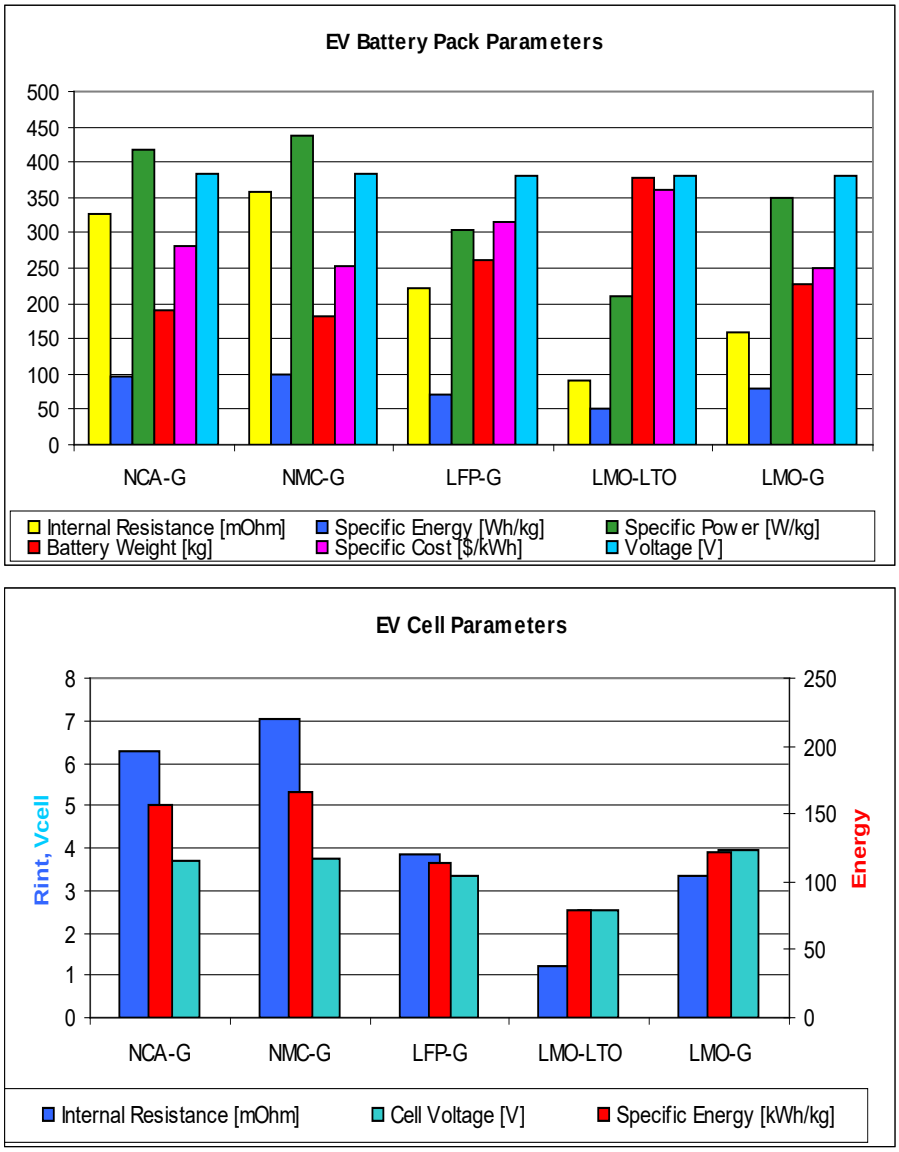

Figure 10: Typical EV battery pack (24 kWh, 67 Ah) and cell parameters for various Lithium-Ion battery types

The NCA and the NMC graphite systems have the highest specific power and energy characteristics. This is due to their high cell voltage and good electrode specific capacities relative to other Lithium-Ion types and can thus provide higher driving range for both types of vehicle, EV and PHEV. Nevertheless, these Lithium-Ion types can experience thermal runaway caused by exothermic reactions (M. Wohlfahrt-Mehrens, 2009), which can lead to dangerous situations (explosion) if they go out of control. Projections show that maintaining the SOC in a reasonable range they would have a good life but work must be done to increase the useful fraction of the SOC range and, at the same time, achieve the requested battery life (P.A. Nelson K. A.).

The results show that among the anode graphite-based battery types, LMO-G cells present the lowest internal resistance. This characteristic is due to the ability of the three-dimensional spinel structure of the electrode to accommodate more lithium within it (Eriksson, 2001). In term of costs, this type of cells is the most promising. This characteristic is probably due to the absence of nickel and cobalt in the manufacturing process of the cell. Although, LMO-G cells are safer than NCA-G and NMC-G, they still present some safety issues (Lam, 2011). In

order to overcome this problem some manufacturers combined the LMO cathode with a lithium-titanate-oxide (LTO) anode.

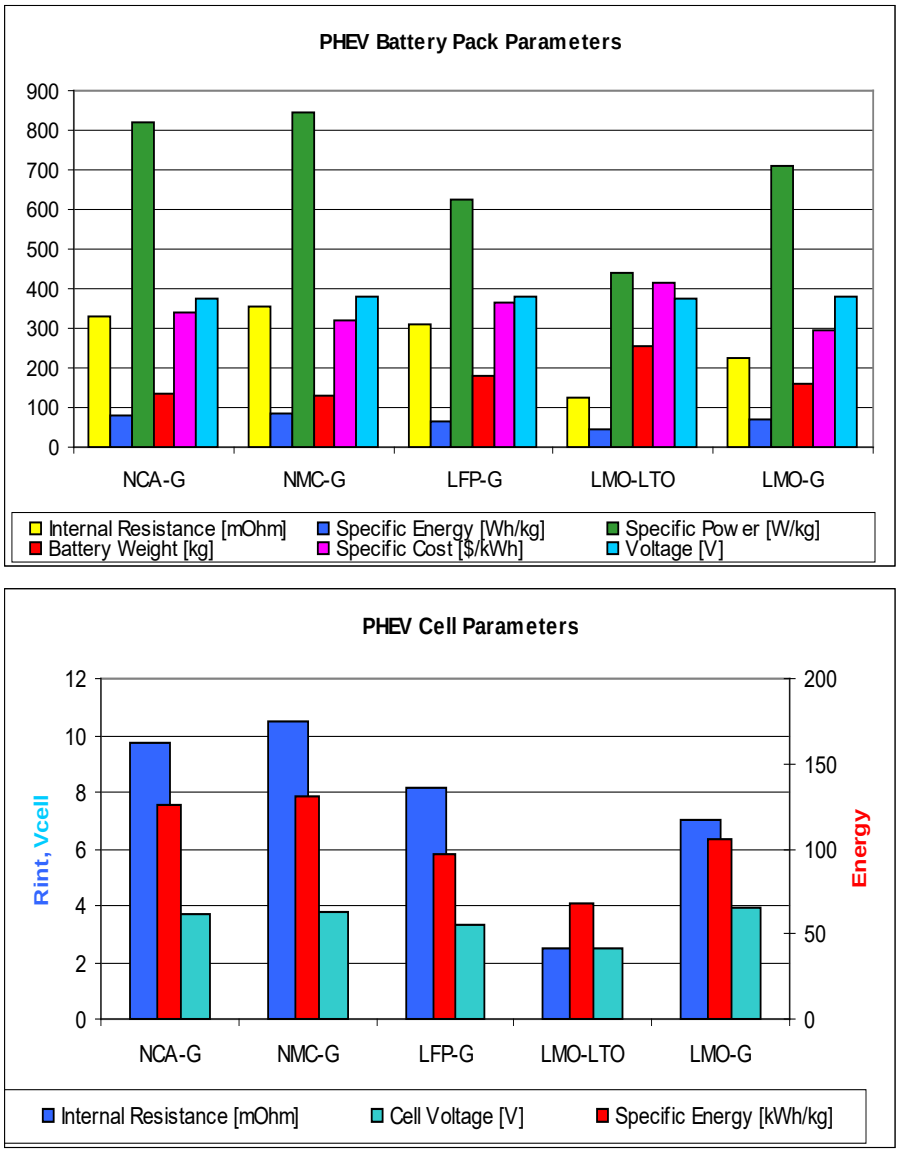

Figure 11: Typical PHEV battery pack (16 kWh, 45Ah) and cell parameters for various Lithium-Ion battery types

As we can see in the results obtained, titanate-based cells (LMO-LTO) have lower specific energy (due to the low cell voltage) than technologies using graphite-based anodes. This characteristic is however associated with a very low internal resistance due to absence of an SEI layer (F.R. Kalhammer, 2009). The absence of the SEI layer is due to the fact that the titanate anode operates at higher positive potential relative to lithium if compared to the graphite anode, precluding the discharge of lithium ions to lithium and the subsequent reaction of lithium with the electrolyte to form the so-called SEI layer. Lacking the SEI layer, also the cycle life of the battery is improved and a high percentage of the battery capacity is available increasing the usable SOC range. Moreover the low internal resistance of this type of cell allows significantly higher charge and discharge rates making this chemistry a promising solution for PHEV applications (F.R. Kalhammer, 2009).

The olivine structure of the cathode is also the reason for the low internal resistance, compared to NCA-G and NMC-G, of the $LiFePO_4$ cells. The key benefits of this type of chemistry are enhanced safety, good thermal stability, tolerance to abuse, high current rating and long cycle life. While the main drawbacks are the low specific energy (due to the low cell voltage), and the poor performances at low temperatures (Lam, 2011).

In this chapter we went through the different Lithium-Ion battery types present in the market today and, thanks to the BatPac model, we analyzed the most important parameters necessary to evaluate the battery characteristics for different pack configuration.
In the next section we will try to better understand what these parameters are and what are the factors that affect them.

4. Factors Affecting Battery Performance

We have seen in the previous chapter the most important parameters necessary to assess and understand the characteristics of a battery system. The internal resistance strongly affects battery performance limiting the specific power, while the capacity strongly affects the specific energy (H.G. Schweiger, 2010). In addition to those the cycling and ageing of a battery also play a big role affecting the battery performance reducing the power and energy available with time.
Besides that, the performance of the battery may be significantly affected by the actual conditions of use, particularly if the battery is used under more stringent conditions than those under which it was characterized. For example the internal resistance of a battery is deeply affected by the temperature and SOC and this effect may have important consequences on the available energy and battery lifetime.
In this chapter we analyze the possible factors that may affect Lithium-Ion battery performance focusing our attention on the losses caused by the internal resistance and how they affect the battery efficiency. In the last section an overview of possible degradation mechanisms and factors affecting battery lifetime will be presented together with an extensive literature review on lifetime battery models.

4.1 Electrochemical Thermodynamics and Kinetics

In Chapter 2 we talked about the definition of a battery and how it stores electricity via chemical reactions. We also defined the terms voltage and capacity, which are both key properties for energy storage. The capacity is a measure of the amount of charge that can be extracted from the battery; the voltage is a measure of the energy contained in the active material of the cell (electrical potential energy).
When the system is in equilibrium we can define the electrical potential energy as Open Circuit Voltage (OCV). When the current starts to flow a resistance will act against the current flow reducing the electrical potential energy of the cell. Some of the voltage will be lost to Joule heating and, as the current flow increases, more and more power is lost in heat instead of producing useful work (Tang, 2010).
The principles and operation of a cell are related with electrochemical processes and thermodynamics. The thermodynamics determine the electrical potential difference between the electrode and electrolyte (and then the OCV of a cell) even in absence of any external circuit. When connecting an external load to the two electrodes, a current starts to flow, and electrode reactions and mass transport begins. These two mechanisms are related to the electrode kinetics and, as seen before, will reduce the potential energy available (Husain, 2011).

4.2 Battery Losses and Internal Resistance

In the previous section we have seen that the chemical driving force across the cell is due to the difference in the chemical potentials of its two electrodes (OCV), which is determined by the difference between the standard Gibbs free energies, the products of the reaction and the reactants. However, the theoretical open circuit voltage is not available during use. As soon as current starts passing through the battery, it runs into an internal resistance. The total

voltage drop caused by the internal resistance is due to a number of different processes and results as a sum of different voltage drops:

$$V_{cell} = V_{OCV} - V_{diff} - V_{ch,tr} - IR_{ohm}$$

The cell voltage V_{cell} under load is governed by the open circuit voltage V_{OCV}, the voltage drops caused by concentration polarisation V_{diff} and charge transfer polarisation $V_{ch,tr}$ as well as the voltage drop caused by internal ohmic resistance, IR_{ohm} (H.G. Schweiger, 2010).
Figure 12 shows that all these voltage drops, due to chemical kinetics, reduce the OCV of the battery affecting the available energy, which will be lower than its theoretical value.

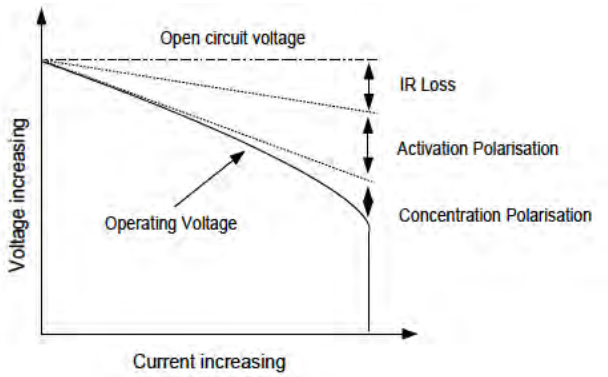

Figure 12: Cell polarization curve (Tahil, 2010)

The *charge transfer polarization*, or *activation polarisation,* is due to the retarding factors that are inherent part of all electrochemical reactions (i.e. $Li \rightarrow Li^+ + e^-$ at the anode and $Li^+ + e^- \rightarrow Li$ at the cathode). These processes consume energy and therefore will cause a voltage drop: $V_{ch,tr}$.
Concentration polarisation is an effect caused by the different concentration of the reactants at the electrode surface, which interfere with the diffusion of ions. The higher the concentration gradient, the higher is the resistance and as a consequence the voltage drop V_{diff} within the cell.
The resistance of the electrolyte (inversely proportional to the electrolyte conductivity), as well as the resistance of the electrode materials, terminals, interconnections, electrode-electrolyte contact area, and other components is the main factor that causes the Ohmic voltage drop within the electrochemical cell, the IR loss.

4.3 Internal Cell Impedance Parameters

In the previous sections we have seen that the internal resistance of a battery takes into account several phenomena.
According to (L. Guzzella A. S., 2007), the internal resistance is a combination of three factors. The ohmic resistance in the electrolyte, electrodes, as well as other battery components is the ohmic resistance R_{ohm}, the resistance associated to the activation reactions at the electrode/electrolyte interface is the charge-transfer resistance $R_{ch,tr}$, and the third resistance is the diffusion resistance R_d, which is due to the ion diffusion within the electrolyte:

$$R_i = R_d + R_{ch,tr} + R_{ohm}$$

The value of the internal resistance is dependent of many parameters such as SOC, discharging or charging C-rate and temperature.

Long Lam developed a practical circuit-based model for EV Lithium-Ion cells in his MSc Thesis (Lam, 2011). The model consists of empirical equations, extracted from measurements on numerous $LiFePO_4$ (A123Systems APR18650M1, 1.1 Ah, 3.3 V) cells tested under possible real operating conditions. The influence of different temperatures (range: -15 – 40°C), SOC, and C-rates, on the discharging and charging behaviour of the cells is modelled. The circuit is split into an energy balance circuit and a voltage response circuit. The energy balance circuit models the self-discharge, the cell capacity, the amount of energy left in the cell and the battery degradation. The voltage response part describes how the cell voltage responds to a given load current. In order to study the internal impedance parameters, in this thesis, we are considering exclusively the voltage response circuit, omitting the energy balance part.
The interesting feature of the model from our point of view is its ability to relate the different influences on the electrochemical processes shown above to the correct circuit components. The voltage response circuit consists of one ohmic resistance (R0) and two parallel RC pairs in series.

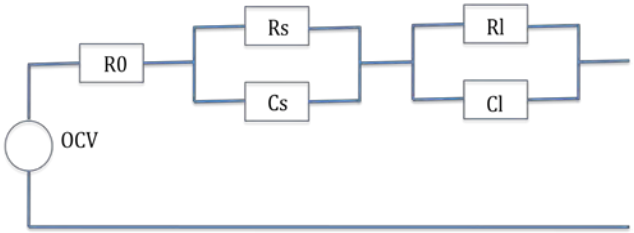

Figure 13: Voltage-response circuit of the Lam model

The open circuit voltage is a voltage source depending on the SOC. The ohmic resistance of the battery cell is given by R0. Rs and Cs represent short time constants in the voltage response and are related to the charge transfer resistance, $R_{ch,tr}$, and the double layer capacitance C_{dl}. The long time constants are accounted for by Rl and Cl, which are linked to a single RC pair modeling the diffusion phenomena.

We implemented this model in an Excel spreadsheet in order to study the behaviour of the various contributions to the internal resistance as a function of temperature and SOC. In the following section the obtained results are presented.

Since the impedance parameters are essentially representations of electrochemical reactions and transport processes inside the battery, they are strongly affected by the internal temperature and the state of charge of the battery. The internal resistance of the battery, represented by the three different resistances seen above, is high at low temperature and drastically decreases as soon as the temperature increases. This is valid for the entire SOC range and for all the three resistances under investigation.

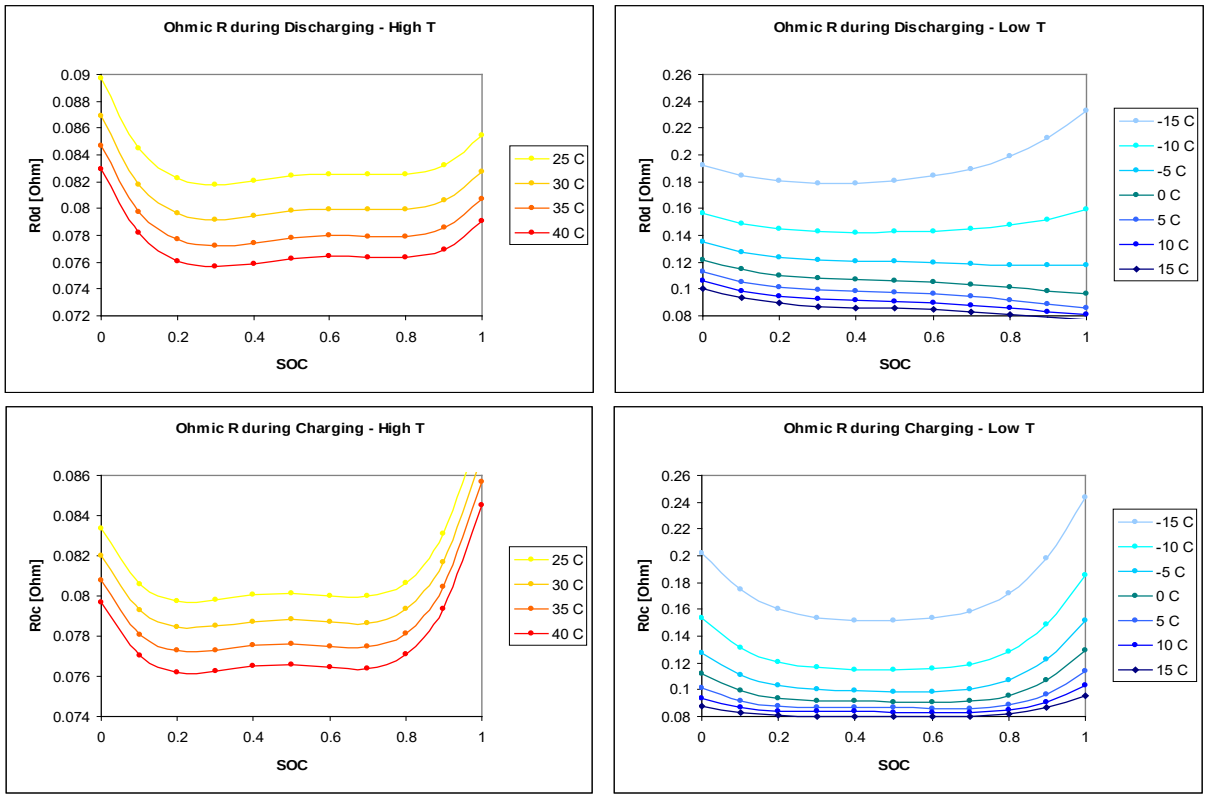

Figure 14: Ohmic resistance trend during discharging (top) and charging (bottom) conditions at high (left) and low (right) temperatures

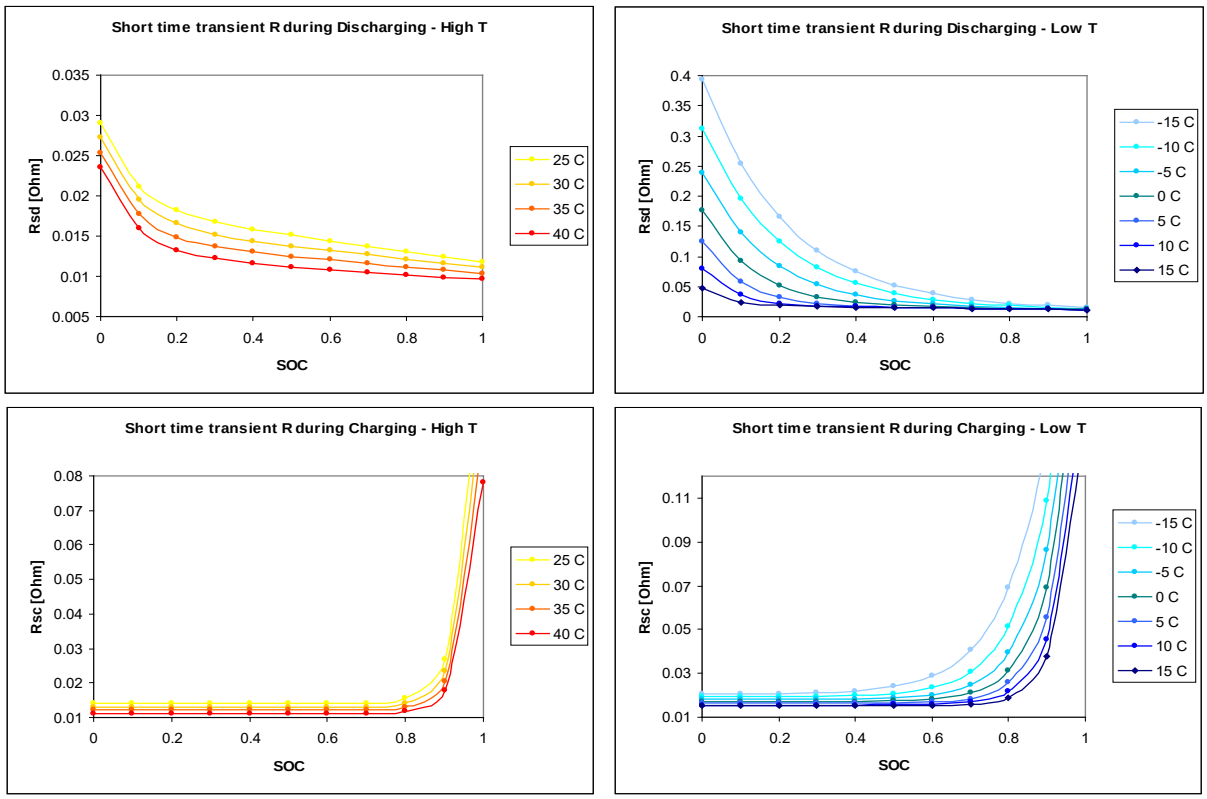

Figure 15: Charge transfer resistance trend during discharging (top) and charging (bottom) conditions at high (left) and low (right) temperatures

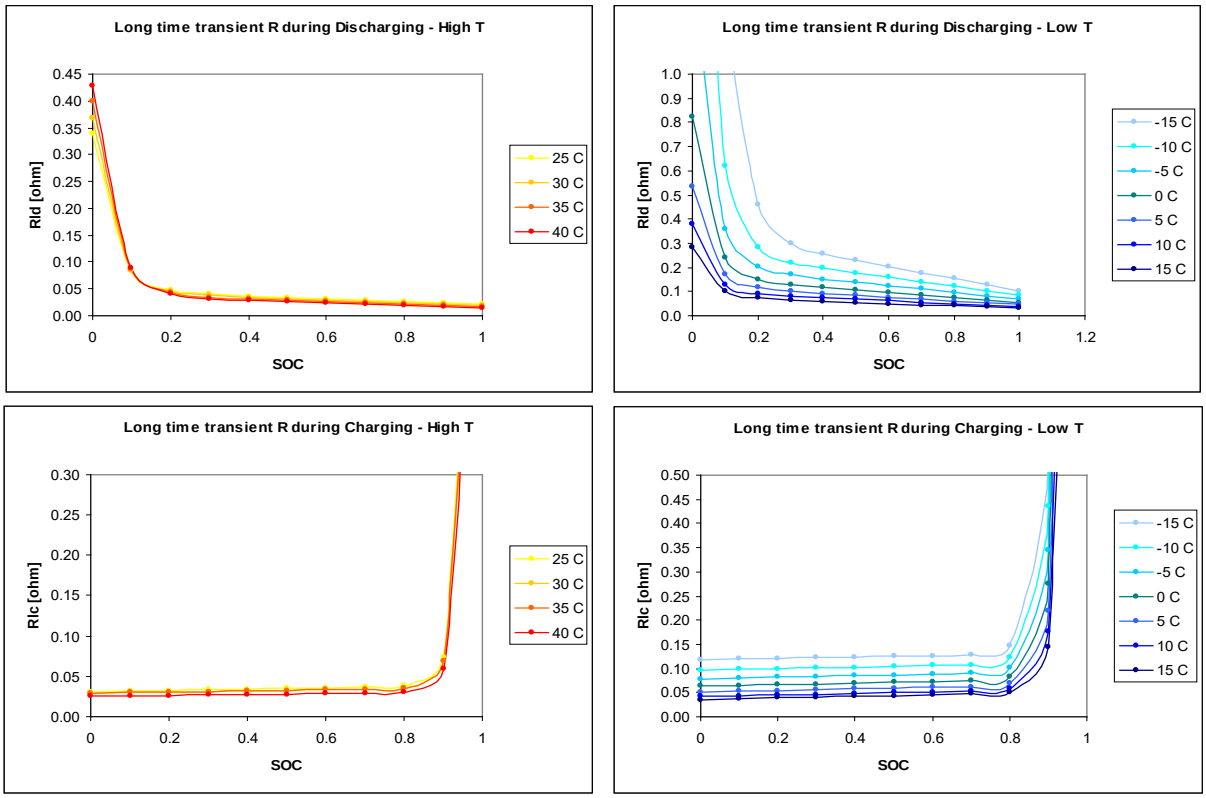

Figure 16: Diffusion, or concentration, resistance trend during discharging (top) and charging (bottom) conditions at high (left) and low (right) temperatures

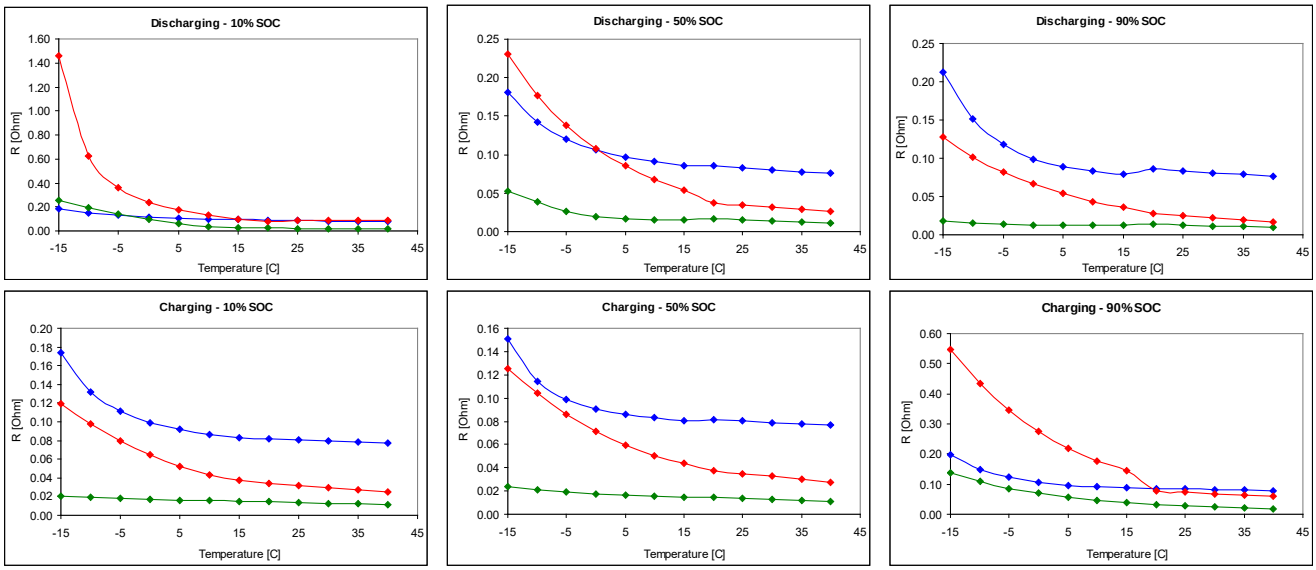

Figure 17: Ohmic (blue), charge transfer (green) and diffusion (red) discharging and charging resistances trend at different SOC conditions as a function of temperature

At high temperature the activation energy of the chemical reactions at electrodes-electrolyte interface is lower and reaction rate higher. This leads to faster intercalation and deintercalation of lithium ions within the cell. High temperature involves also higher diffusion rate of lithium ions in the electrolyte, increasing the current flow. This increment in ion mobility at high temperatures, as we can see in Figure 17, is related to the decrease of the ohmic and diffusion resistances at high temperature. The direct consequence of these effects is a higher

power capability (Lam, 2011). Despite this positive effect, operating the cell at high temperatures has its own drawbacks. The cell may be severely damaged, due to an increased degradation rate of the SEI layer (J. Vetter, 2005), and its life drastically reduced due to the highest self-discharge rate of the batteries at high temperatures.

At low temperatures the opposite holds. The higher activation energy needed to activate the intercalation and deintercalation processes, together with a lower diffusion rate of lithium ions within the electrolyte, result in an increase of ohmic and diffusion resistances, which cause a loss of power. So the poor performance of Lithium-Ion cells at low temperatures is in part due to poor electrode kinetics (S.S. Zhang, 2003).
Due to the strong influence that the temperature has on battery performance and lifetime, Lithium-Ion cells have an optimal temperature operating range, usually specified by the manufacturers (i.e. GAIA HP 601300, 27 Ah NCA-G cell has an operating temperature range of -30°C – 60°C).

We already mentioned that temperature, SOC, C-rate and other factors have a strong influence not only on battery performance but also on battery lifetime. The lifetime of a battery is very important, since it is the most costly part of an electric-drive vehicle. A literature review on the causes affecting the lifetime and its modeling has been done in this thesis and will be presented in the next subsection.

4.4 Battery Lifetime

The arrival of electric vehicles into the automotive market over the past decade and its continued growth has required the introduction of new rules and requirements. The European Commission and state governments in Europe, USABS (a consortium formed by the US DOE together with various national laboratories and the major US auto makers) in the USA, and CRIEPI in Japan, have developed requirements for electric drive vehicles, which also include an expected life of the battery system.
Due to their extreme importance on battery performance, we considered it important to assess the degradation factors affecting the battery lifetime even if they are not further evaluated in this work.

Degradation in Lithium-Ion batteries is mainly caused by an increase of the internal resistance and a reduction in capacity with time. The consequences on battery performance are reflected by a reduction of the available energy and power with increasing storage time, and number of cycles. Furthermore, battery degradation can be accelerated with the DOD, cycling frequency and high temperatures (K. Smith, 2012).

Capacity decrease and power fading are not caused by a single factor but a number of different processes are involved. Vetter, Novak et al. (J. Vetter, 2005) give a review of the knowledge on the aging mechanisms in Lithium-Ion batteries identifying and evaluating different processes that are involved, and classifying them according to the electrode that is experiencing the aging process.

For an in-depth study of these factors a good knowledge of chemistry is required and is not the purpose of this work. In the next steps only a schematic overview of the problem related with aging is given.

4.4.1 Ageing of Anodes

Vetter, Novak et al. (J. Vetter, 2005) claim that anode "*ageing with time and use can lead to, and may be caused by changes, which can occur at the electrode/electrolyte interface (affecting both electrode and electrolyte), active material, and composite electrode*".
Between those, the one affecting the electrode/electrolyte interface are considered to play the most relevant role in the ageing process of the anode.
The dominant anode ageing mechanisms, causes and effects are shown in Figure 18 and summarized in the following table:

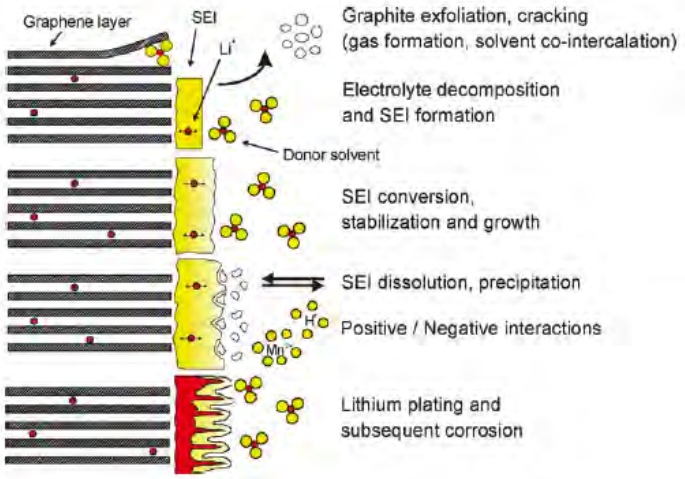

Figure 18: Changes at the anode/electrolyte interface (J. Vetter, 2005)

SEI formation		
- Electrolyte decomposition	Loss of lithium Impedance rise	Capacity fade Power fade
SEI growth		
- Decrease of accessible surface area	Impedance rise	Power fade
- Volume changes	Impedance rise Overpotentials	Power fade
Volume changes		
- Contact loss of active material	Loss of active material	Capacity fade
Metallic lithium plating		
- Electrolyte decomposition	Loss of lithium Loss of electrolyte	Capacity Power fade

Table 3: Anode ageing mechanisms, causes and effects. Based on (J. Vetter, 2005)

4.4.2 Ageing of Cathodes

As well as for the anode, also the degradation of the cathode may affect the battery performance with time and cycle number. With respect to the cathode, however, we should consider the different compositions (while for anode ageing we just considered carbonaceous anode) because the ageing of the electrode is very sensitive to individual compositions. Despite that, in general, capacity fading of positive electrode active material can originate from three basic mechanisms, which are shown in Figure 19 and listed below (J. Vetter, 2005):

- Structural changes during cycling;
- Chemical decomposition/dissolution reaction;
- Surface film modification.

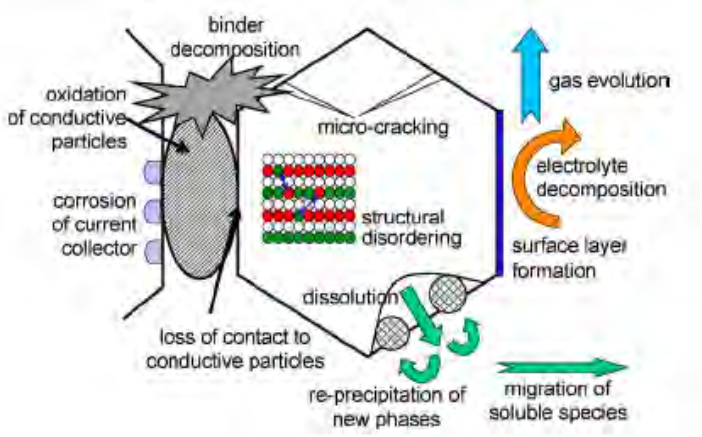

Figure 19: Overview of basic ageing mechanisms at cathode (J. Vetter, 2005)

4.4.3 Summary of Ageing

Many and complex mechanisms are at the origin of the cell degradation. These mechanisms can be accentuated by different operating conditions such as high and low temperatures and SOC, and are strongly related with the battery chemistry. They lead to a growth of internal impedance and capacity decrease, which cause performance degradation with increasing cycling and storage time (J. Vetter, 2005).
Manufacturers usually specify the degradation characteristics of the Lithium-Ion cell under ideal conditions. Conditions are however almost never ideal in real life applications, especially in EV and PHEV applications. Non-ideal conditions in general will accelerate the capacity fading and cause additionally cell life decay. Due to these, and other technical and economical reasons (batteries are often the most expensive component of electric-drive vehicles), battery lifetime prognosis is a key requirement for successful market introduction of electric and hybrid vehicles and the questions related to battery lifetime prediction and management has become more and more significant.

4.5 Battery Lifetime Modeling: literature review

Due to the high cost of automotive battery packs, it is cost prohibitive to run aging experiments (which would deteriorate the battery) across a wide range of possible drive cycle, charging scenario, and temperature conditions. Despite cell experiments being performed in a laboratory environment, the need of accurate and reliable battery lifetime models is growing hand in hand with the development of the EV market.
Degradation factors affecting battery lifetime are modelled and various models are present in the literature. Due to the fact that degradation in Lithium-Ion batteries is mainly caused by an increase of the internal impedance and a reduction in capacity, the common approach is to model these two parameters as a function of time, and other parameters such as DOD, cycling number and temperatures.
The aim of this section is to try to get an insight on how these factors are modelled even if they are not considered afterwards in our simulation.

What is interesting to point out from this literature research is that the only degradation parameter common to all models is the temperature: the dependence of the degradation on the temperature can be modelled with the Arrhenius equation (Millner, 2010), (Spotnitz, 2003), (B.Y. Liaw, 2003):

$$A = A_0 \cdot e^{-\frac{E_a}{RT}}$$

Where A is the quantity of interest, A_0 the pre-exponential term, E_a the activation energy, R the gas constant and T the temperature in Kelvin. The activation energy was found to be dependent on the SOC at which the cell was kept at during ageing and the duration of the ageing (B.Y. Liaw, 2003). At high SOC, the activation energy is lower than for low SOC, and the E_a lowered with increasing ageing time. This means that unwanted reactions will occur more easily at high SOC and the amount of degradation will increase with increasing capacity fading.
An interesting point comes out from this analysis. Lithium-Ion battery degrades more easily if left at high SOC and high temperature. This means that, in order to protect an EV battery from a faster degradation, it is more convenient to park the car at low temperatures and low SOC.

As mentioned before, apart from the temperature, battery manufacturers and researches do not have a common method to model all the other degradation factors (such as DOD, cycle numbers, voltage, etc…). Some of them include only a few factors in their analysis, considering others negligible, and none of them include all. It is also very hard to find a common agreement on the dependence of the resistance growth and capacity fading from one of the degradation factors. For example Ecker et al. (M. Ecker, 2012) developed a lifetime model able to evaluate the effect of temperature and SOC on impedance rise and capacity fade. As we can see in Figure 20, both mechanisms are $t^{1/2}$ dependent, while in Smith et al. (K. Smith, 2012) model, developed at NREL, both mechanisms in addition to this factor also includes a linear component of time and cycle number.

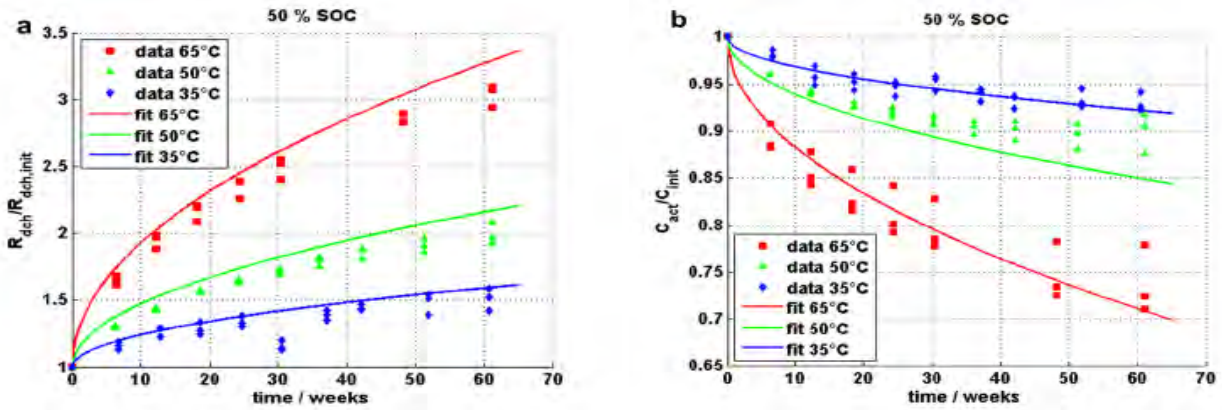

Figure 20: Fitting results for a) resistance increase (actual resistance normalized to initial resistance) and b) capacity fade (actual capacity normalized to initial capacity) over time (M. Ecker, 2012)

5. Battery Cell Modeling

In order to understand the effect of a constant discharging/charging rate and temperature on energy and power capability, simulations have been performed.
This chapter begins with a brief introduction on the different type of battery models used by battery manufacturers and researchers with a focus on electrical models. Equivalent circuit models are the most common approach for EV battery simulation and are the type of model used in this work. In section 5.2 the equivalent circuit model used for the analysis of the energy capability of two different battery cells (NMC and LFP) is introduced and the results obtained from the simulation are shown. In the last section the discharging and charging power capability of the two cells, as a function of SOC and temperature, is presented.

5.1 Background

Laboratory tests and measurements, especially for large batteries, are expensive and time consuming. In order to reduce cost and time, battery simulation has become, in recent years, a practice increasingly used by battery manufacturers and researchers.
In the literature a wide variety of battery models with varying degrees of complexity is present. M. Chen and G. Rincon-Mora (M. Chen, 2006) give a detailed classification of the different types of models. They classify the models as follows:

- *Electrochemical models*: mainly used to optimize the physical design aspects of batteries, are in general complex and not easy to link with other system models (i.e. vehicle model).
- *Mathematical models*: are in general complex and computationally intense.
- *Electrical models*, which are represented by equivalent circuits where voltage sources, resistors and capacitors simulate the physical behaviour of the battery. They can be easily implemented with other systems.

Electrical models can be classified based on the number of RC connection they have. For Lithium-Ion cells the most common choice is to connect one or two RC block with a series resistance. Figure 21 shows the three possible types of circuit-based model used for analysis of Lithium-Ion cells. The components represented in all the three models are the OCV and the ohmic resistance R_0 (representing the resistance of the contacts, the electrodes, as well as the electrolyte). The other parameters: R_1, C_1, R_2 and C_2 characterize the transient response of the battery and are in general related with the other electrochemical processes within the cell (i.e. diffusion, charge transfer, etc.).

5.2 Energy Capability Analysis

In this section the energy capability dependency on different temperature, discharging currents and battery types has been analyzed. First, a single RC block model able to simulate the discharging dynamics of a single NMC cell has been used and the energy characteristics of the cell at different temperature and discharging C-rate analyzed. Then, an additional RC block was added to the existing circuit model and different parameterization values suitable for an LFP cell, able to characterize the impedance parameters at lower temperatures, were used.

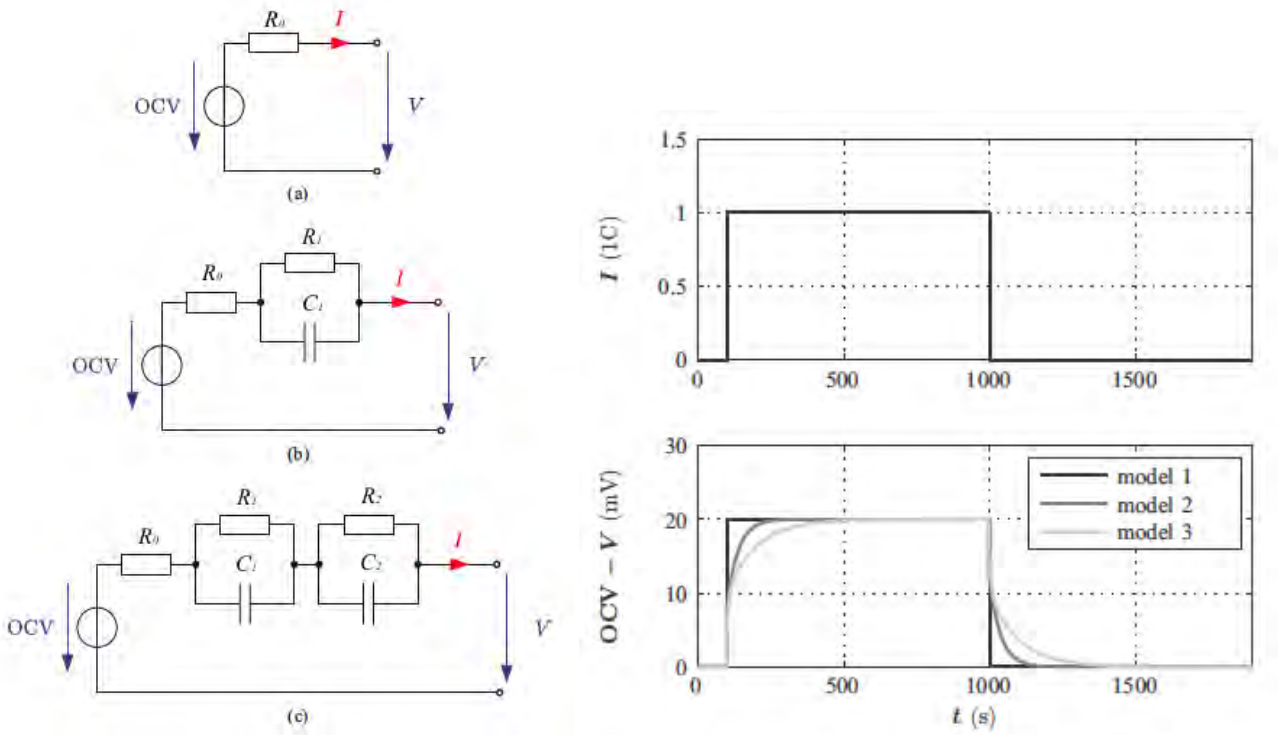

Figure 21: Basic electrical battery models with (a) one R, Model1. (b) one R and one RC combination, Model2. and one R and (c) two RC combinations, Model 3. On the right, voltage response when a rectangular current pulse of 1C is applied to the battery impedance of each model (M. Einhorn, 2013)

5.2.1 Model Formulation

In order to analyse the effect of a varying discharging current at different temperatures on cell energy capability, the model developed by Huria et al. (T. Huria, 2012) has been adopted in this work. The single RC block model with numerical parameter estimation scheme using tests on NMC cells under different operating conditions was implemented using MATLAB, Simulink and Simscape. The tests performed on NMC cells revealed the dependencies of the model parameter (OCV, series resistance and RC block) on temperature and SOC. These dependencies were implemented into the model as a two-dimensional lookup tables that determine the values of each circuit elements during the simulation stage at three different temperatures (5, 20 and 40 degrees) and different SOC (0, 0.1, 0.25, 0.5, 0.75, 0.9 and 1).
Since we want to analyze the energy and power capability of the cell at fixed temperature, the thermal effects of the convective heat exchange between the cell and the environment are not considered and the input temperature of the battery is constant over the charge/discharge cycle.
Figure 22 and 23 show the Simulink blocks used for the simulation. The input parameters of the simulation, charging/discharging current and temperature, are depicted with green blocks in Figure 22. Based on the SOC, current and temperature at time t, the cell model is able to set the impedance parameter values (lookup tables) necessary to calculate the dynamic of the battery and gives the output values, which will act as inputs for the following iteration.

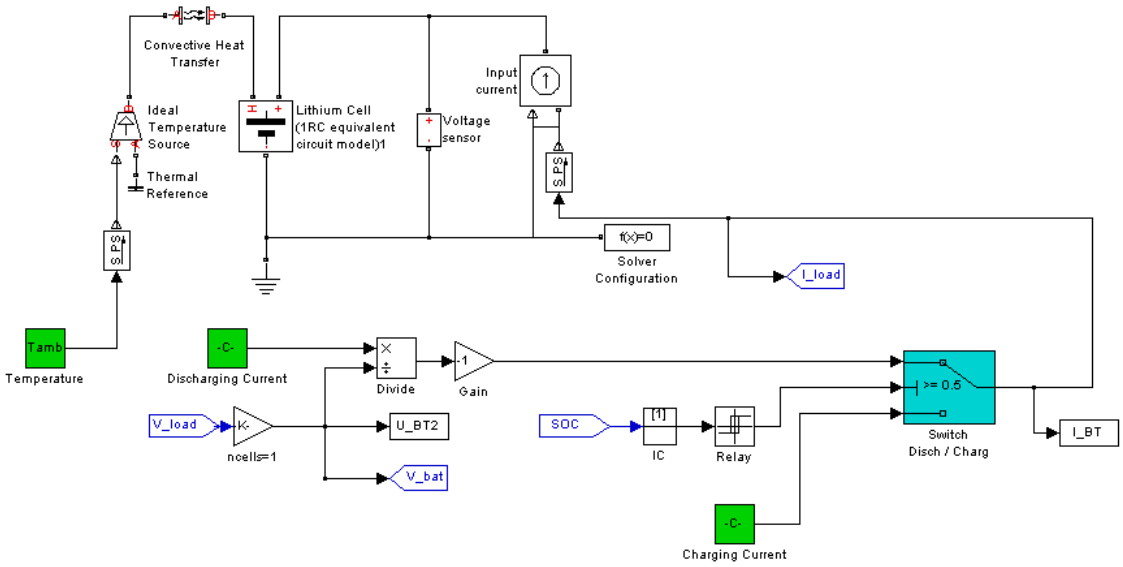

Figure 22: Simulink scheme of the battery cell with charging/discharging interface and convective heat exchange with the environment

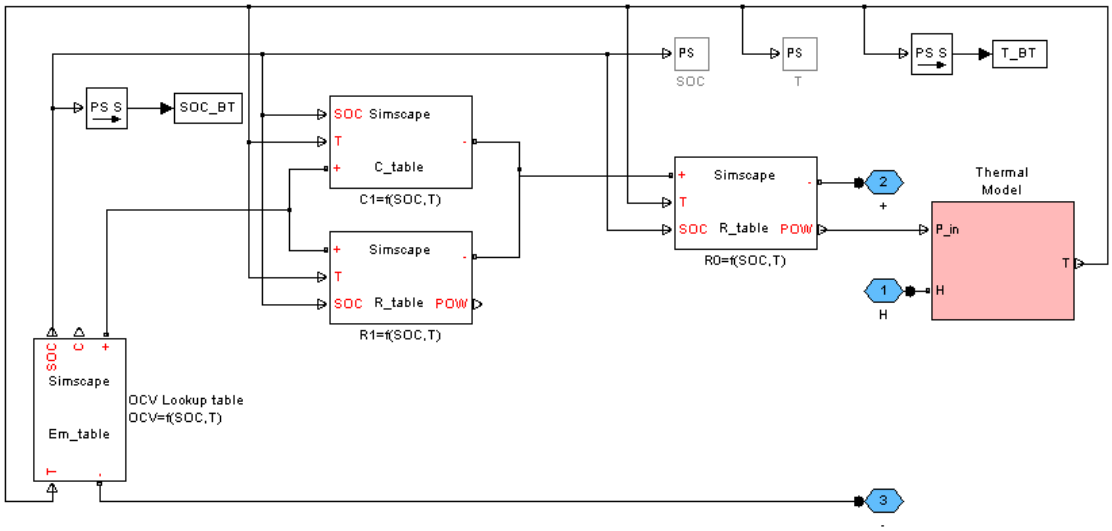

Figure 23: Simscape representation of the cell using one RC element in series with an internal resistance

In order to analyse the effects of the C-rate on the available energy at lower temperatures (no measurements performed below 5°C for the cell adopted in (T. Huria, 2012)) we implemented a two RC blocks circuit that uses the impedance parameters for LFP-G cell from section 4.3 (Lam, 2011) (for which impedance measurements down to -15°C were done), and we run the same simulation as before.

5.2.2 Simulation Results and Discussions

Using the model introduced in the previous section, we performed the simulation at different temperature and discharge current for the two battery chemistries considered. For the NMC type the C-rate range is varied from $\frac{C}{10}$ to $2C$, and the temperature from 5° to 40°C. For the

LFP battery the simulated temperatures are lower (from -15° to 20°C) while the C-rate range is the same as for the NMC battery.
The SOC range in which the simulation is performed is 0.1-0.9, which is a realistic range for EV applications.
The power of the battery is calculated during the discharging phase as follows:

$$P_{BT} = I_{BT} \cdot V_{BT}$$

While the energy available during the discharging phase is calculated by integrating the power over time during the discharging phase:

$$E_{disch} = \int_{t \in t_{disch}} P_{BT} dt$$

The simulation results for the different batteries used are shown in the following figures. Figure 24 (left), shows the available energy at different C-rates and temperature for a NMC battery type calculated using a single RC element in series with an internal resistance while Figure 24 (right), shows the same results obtained for a LFP battery using two RC element in series with the internal resistance.

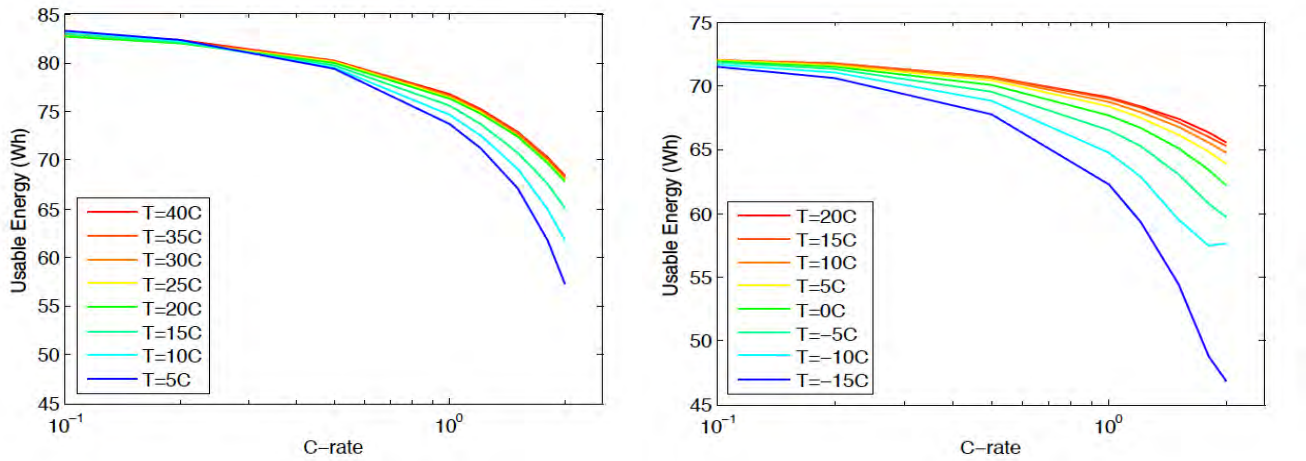

Figure 24: Usable energy vs. C-rate at different temperature for NMC cell (left) and LFP cell (right)

In figure 24 we can see that the usable energy depends on the C-rate and temperature of the battery for both chemistries analyzed. However, considering the same temperature range for both chemistries (between 5°C and 20°C), the energy drop found for the NMC type is higher compared to the one we have found for the LFP cell type. This is mainly due to the higher internal resistance values of the NMC. Higher internal resistance means a higher voltage drop and a higher voltage drop means less available energy.
Concerning the temperature dependence, as we can easily see in Figure 24 left, the energy capacity is not really temperature dependent for temperature higher than 20°C. In this range only the C-rate has consequences on the usable energy of the cell. This is not true for temperature below 20 degrees when we can start to see a slight temperature dependence, which strongly increases as the temperature gets lower and lower (Figure 24 right). The large energy drop at low temperature is due to the high values of the internal resistance, particularly for temperatures below zero, as we have previously seen in section 4.3.

5.3 Power Capability Analysis

Discharge and charge power capability are defined from the voltage and resistance characteristics (temperature and SOC dependent) as well as from the maximum voltage (during charging) and the cut-off voltage (during discharging) at each SOC analyzed (IDL, 2008):

$$\text{Discharge Power Capability: } P_{disch} = V_{cut-off} \cdot \left(\frac{V_{OCV}(SoC,T) - V_{cut-off}}{R_{disch}(SoC,T)} \right)$$

$$\text{Charge Power Capability: } P_{ch} = V_{\max} \cdot \left(\frac{V_{\max} - V_{OCV}(SoC,T)}{R_{ch}(SoC,T)} \right)$$

Discharge and charge power capability values versus SOC are plotted in Figure 25 for the NMC cell and in Figure 26 for the LFP cell. The values on the secondary axis are the power values normalized to the rated power at SOC=0.5 and T=20°C.

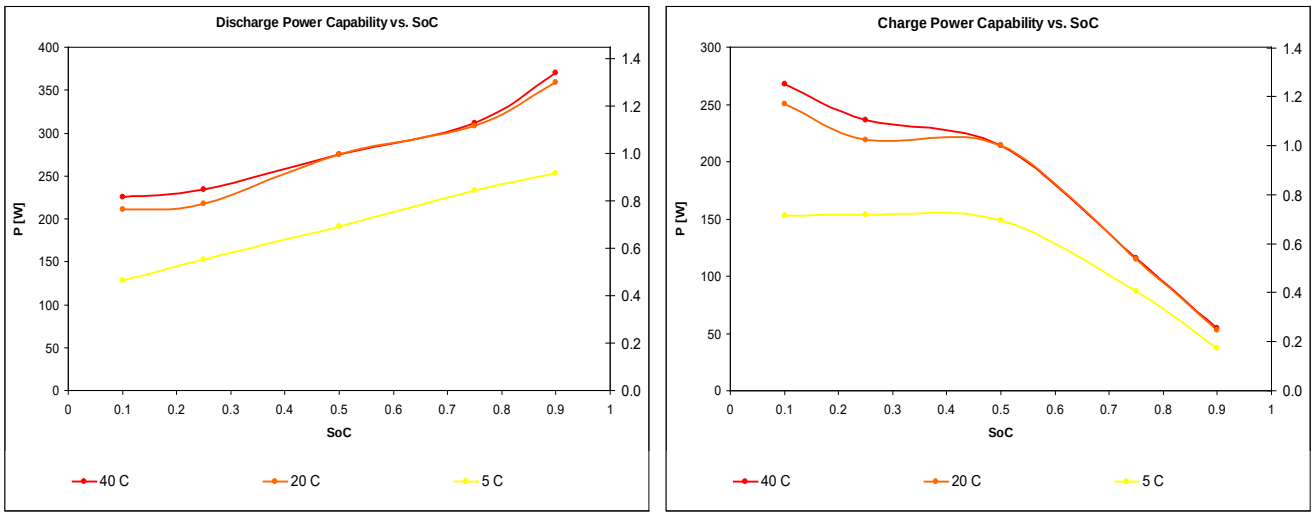

Figure 25: Discharge and charge power capability vs. SOC for NMC cell, 31Ah, 3.7 V.

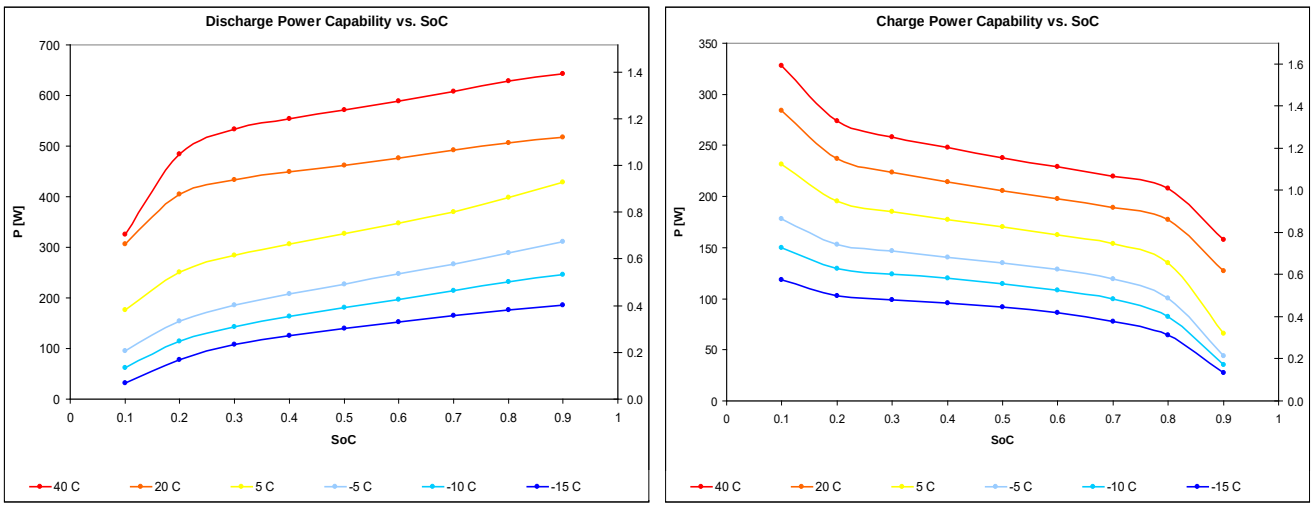

Figure 26: Discharge and charge power capability vs. SOC for LFP cell, 31 Ah, 3.3 V

6. Electric Vehicle Modeling

In this Chapter the battery implementation into a vehicle model and how different charging/driving conditions may affect battery efficiency is assessed. First a brief introduction of the vehicle model used is given, and then battery efficiencies in different charging and driving conditions are evaluated. Since the time and efficiency of battery charging are becoming increasingly important parameters, particular emphasis is given in the analysis of the efficiency and power loss during fast charging conditions. The Chapter concludes with an analysis of traction and regeneration efficiencies when different driving cycles are performed.

6.1 Vehicle Model

In this section the model, which describes the longitudinal dynamic effects of the vehicle is introduced. This is important because in the considered Simulink simulation the forces acting on the vehicle for a specific driving cycle are the inputs to the powertrain of the vehicle, and thus, they represent the load on the battery system.

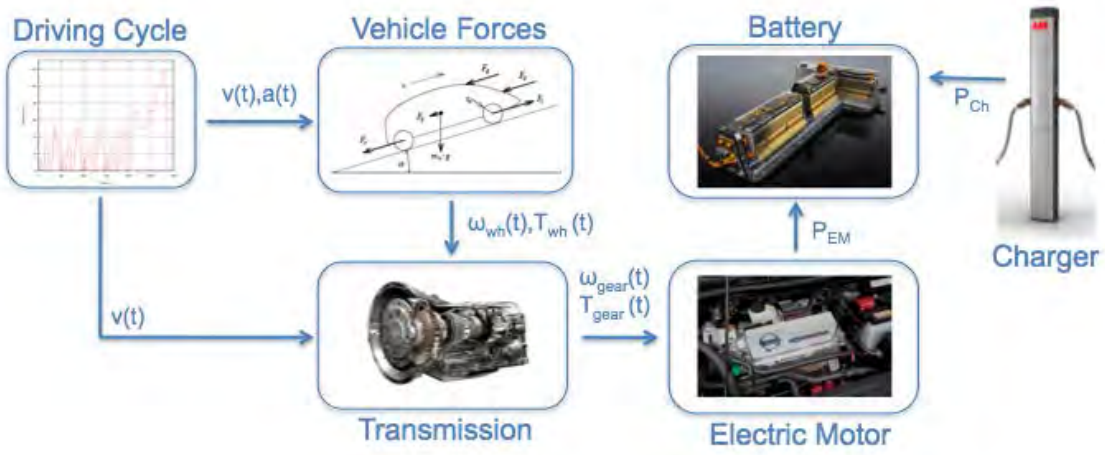

Figure 27: Vehicle model schematization

The elementary equation that describes the longitudinal dynamics of a road vehicle and the forces acting on it, are shown in Figure 28 and explained in (L. Guzzella, 2007).

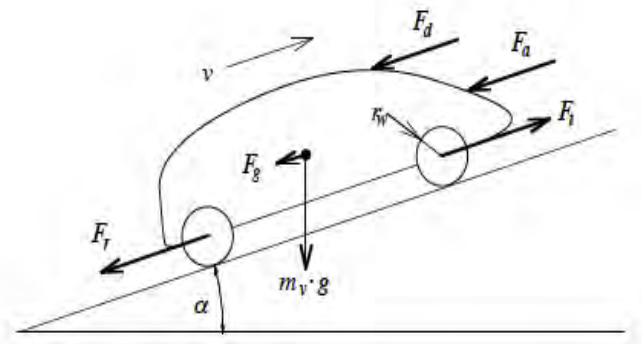

Figure 28: Schematic representation of the forces acting on a vehicle in motion (left), and fundamental equation governing vehicle dynamics (right) (L. Guzzella A. S., 2007)

$$m_v \frac{d}{dt} v(t) = F_t(t) - (F_a(t) + F_r(t) + F_g(t) + F_d(t))$$

Where:

$$F_t = 0\_ : coasting$$

Traction force: $F_t < 0\_ : braking$

$$F_t > 0\_ : traction$$

Aerodynamic drag: $F_a(t) = \frac{1}{2} \cdot \rho_a \cdot A_f \cdot c_d \cdot v^2$

Rolling friction: $F_r(t) = c_r \cdot m_v \cdot g \cos(\alpha)$

Hill climbing force: $F_g(t) = m_v \cdot g \sin(\alpha)$

Disturbance force: F_d

In our simulation approach, the input variables are the speed v, and the acceleration a, of the vehicle. The angle α is always zero. With this information, the traction force that has to be acting on the wheels to drive the chosen profile for a vehicle described by its main parameters (A_f, c_d, c_r, m_v) is computed.
To perform vehicle simulation, in this thesis is used the QSS Toolbox (L. Guzzella A. A., 2005) developed at ETH Zurich.
As we could see in Figure 27, the battery receives inputs from the different load conditions (particularly from the velocity of the car, which determines the current into the battery) and from the charger (different charging powers) during the charging phase. In the next two sections we analyze, using the QSS Toolbox with the battery seen in Chapter 5, how these two different conditions may affect the power loss of the battery.

6.2 Battery Power Losses during Charging

Electric and plug-in hybrid vehicles need electricity in order to charge their battery. Since the market of EV and PHEV is expanding, there is a growing need of charging stations. Although most EV can be recharged at home using a domestic wall socket, there are also other methods available to charge the battery. These methods differ from each other according to the charging power, time and location. In Table 5 the different charging methods are listed together with the main parameters involved (Groll, 2012). This classification is shown in order to give a general idea about the possible charging methods and power involved. A better definition of the so-called *charging modes* is given in the international standard IEC 61851-1 (IEC, 2001).

Charging Method	Power Supply	Voltage	Charging Time
Home Charging	3.3 - 3.7 kW AC/SP 11 kW AC/TP	230 V / AC 400 V / AC	6-8 hours 2 hours
Workplace Charging	11 kW AC/TP 22 kW AC/TP	400 V / AC 400 V / AC	2 hours 1 hours
Public Parking Charging	22 kW AC/TP	400 V / AC	1 hour
Fast Charging	43 kW AC/TP 50 kW DC	400 V / AC 400-500 V / DC	30 minutes 30 minutes

Table 4: Charging methods (AC: Alternating Current, DC: Direct Current, SP: Single Phase, TP: Three Phases)

6.2.1 Fast Charging

The possibility to fast charge the battery reduces the refuelling time extending the practical daily range of EV and therefore making them more competitive with ICE vehicles (A. Burke, 2012).
DC fast chargers deliver electricity directly to the battery (bypassing the AC/DC converter inside of the car) at a higher rate than other chargers would allow. This kind of system may offer a restricted charge (typically up to 80% SOC) or require a lower charging rate after that 80% SOC is reached in order to avoid damage to the battery (Bullis, 2012).
In recent times particular attention has been given to fast charging to the point that Companies dedicated to this purpose are being born worldwide. CHAdeMO is probably the most important among them. CHAdeMO is *"a trade name of quick charging method that this association is proposing globally as an industry standard"* (CHAdeMO, 2010). The

association, formed by TEPCO and the major Asian car manufacturers, installed (up to September 2012) 1693 DC quick chargers worldwide (242 of which in Europe and more than 1300 in Japan). The positive effects of the installation of DC fast charger (up to 500 V/DC and 125A) are resumed in a research done by TEPCO (Anegawa, 2009) which states that after introducing fast charging infrastructure in the Tokyo metropolitan area the average monthly distance per EV owner increased from about 200 to 1500 km. Moreover the installation of one DC fast charger increased also the battery charging capacity used by the EV drivers. They feel easy because they can recharge whenever they like reducing the phenomenon described as “range anxiety”.
In order to analyse the effects on energy losses occurring in the battery during charging, a simulation is performed using the QSS Toolbox with an implementation of two different battery equivalent circuits, which have been already introduced in the previous chapter.

6.2.2 Simulation Results and Discussions

Using the model introduced in the previous section, we performed the simulation at different charging powers for the two battery chemistries considered. The charging power is set from 3 to 50 kW, which is the realistic range of the different charging station previously listed and available on the market. The temperature is maintained constant at 20°C and the SOC range is the typical range used for EV applications: 0.1-0.9.
The battery pack (number of cell in series) is configured in such a way to ensure a similar battery pack voltage for both the chemistries involved in the simulation. The same thing is done with the battery capacity.
The battery power and the power loss, during the charging phase are calculated as:

$$P_{BT} = I_{BT} \cdot V_{BT}$$

$$P_{loss} = R_{\text{int}} \cdot I_{BT}^2$$

Where the internal resistance of the battery, as stated in 4.3, is calculated as the sum of the resistances of each circuit block, which are evaluated as a function of SOC and temperature:

$$R_{\text{int}} = R_0 + R_1 + R_2$$

The energy accumulated in the battery during charging is calculated by integrating the power over the charging time:

$$E_{ch} = \int_{t \in t_{ch}} P_{BT} dt$$

The energy lost due to the heating of the battery during the charging phase is:

$$E_{ch,loss} = \int_{t \in t_{ch}} P_{loss} dt$$

With these energies we are able to calculate the charging efficiency as:

$$\eta_{ch} = \frac{E_{ch}}{E_{ch} + E_{ch,loss}}$$

The simulation results for the different batteries used are shown in Figure 29, which shows the battery charging efficiency as well as the average power losses during the charging phase for the NMC-G and LFP-G battery pack.

As expected, results show a quadratic increase of the power loss with increasing charging power. This is of course due to the fact that the power losses during the charge depend on the square of the current ($P_{loss} = R_{\text{int}} \cdot I_{BT}^2$). Consequently the efficiency decreases at high charging power.
In Figure 29 we can also see that the lower internal resistance of the lithium iron phosphate cells leads to a constantly higher efficiency of the LFP battery compared to the NMC. This trend is amplified at high charging power and is particularly important if we consider battery energy losses during fast charging.
As mentioned before, in recent times the possibility to fast charge EV batteries is becoming an important issue, which would allow EV drivers to extend the practical daily range of EV reducing “range anxiety”. With the results obtained, due to its higher efficiency at high power, we can conclude that the LFP chemistry is more suitable to be fast charged than the NMC. Similar results are found by Burke et al (A. Burke, 2012). They tested different Lithium-Ion chemistries summarizing the performance and fast charging characteristics of each cell. They found that the most promising chemistry for fast charging is the lithium titanate oxide, which has a clear advantage over all the other tested chemistries, especially if compared to the NMC. Since the efficiency strongly depends on the internal resistance, we could confirm the same conclusion looking at the results obtained in Chapter 3.4.
Despite that, work has to be done in order to improve battery performance under fast charging conditions, especially for carbon-based anodes. As we have previously seen in this thesis the electrochemical kinetics inside the battery plays a fundamental role in battery performance. In order to enhance the charging (and discharging) performance the kinetics of electrons and ions should be improved. This can be reflected as an improvement in the electron conductivity of the active material as well as in the ion conductivity of the electrolyte.
H. S. Choi and C. R. Park (H.S. Choi, 2010) list a series of solutions to enhance the electron kinetics and ionic conductivity in order to achieve good anode performance at high charging and discharging rate, such as an increment of the accessible surface area of the anode, short diffusion length, and continuity in ion and electron pathways. In order to achieve such goals some forethought in the anode and electrolyte fabrication (i.e. mixing ratio, thickness of electrode) is necessary especially considering fast charging conditions when rapid charge transfer occurs. Furthermore a possible enhancing methodology is to adopt various nanotechnologies.
The utilization of nanotechnologies allowed Braun (P.V. Braun, 2011) and his research team to enhance the ion and electron transport pathways to such an extent to obtain very large battery charge and discharge rates (up to 400 C for Lithium-Ion chemistry) with minimal capacity loss. Using this method Braun states that is possible to fabricate a “*Lithium-Ion battery that can be charged in two minutes”*.

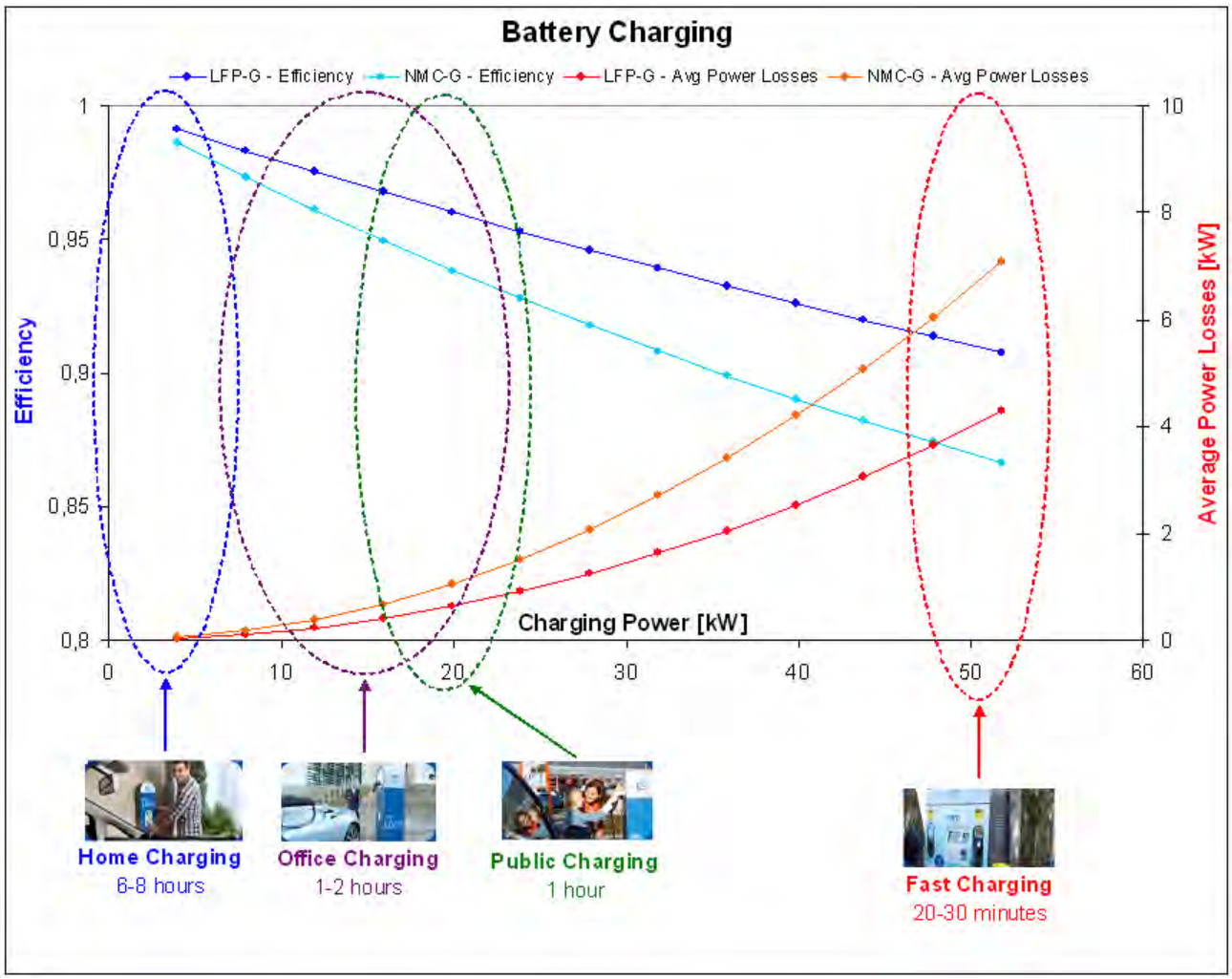

Figure 29: 16 kWh Battery, charging efficiency and average power losses for different charging power

6.3 Battery Power Losses during Different Driving Conditions

After having analyzed efficiency and battery power losses during the charging phase the same is done also for the discharging phase where different driving conditions are assessed. First we considered constant velocity profiles, after those different driving cycles are evaluated and the efficiency of the traction phase together with the regeneration phase (due to regenerative braking) for each driving cycle are calculated.

6.3.1 Average Vehicle Speed

In order to calculate the discharging efficiency and power losses at different velocities we performed the same simulation seen in 6.2.2 but instead of varying the charging power, we let the velocity range from about 50 to 150 km/h. The vehicle considered is a typical mid-size vehicle with a mass of 1500 kg. The efficiency as well as the power losses during the discharging phase are calculated in the same way as was done previously for the charging phase; the only difference is the time range considered which is of course the discharging time rather than the charging time. Results are shown in Figure 30.

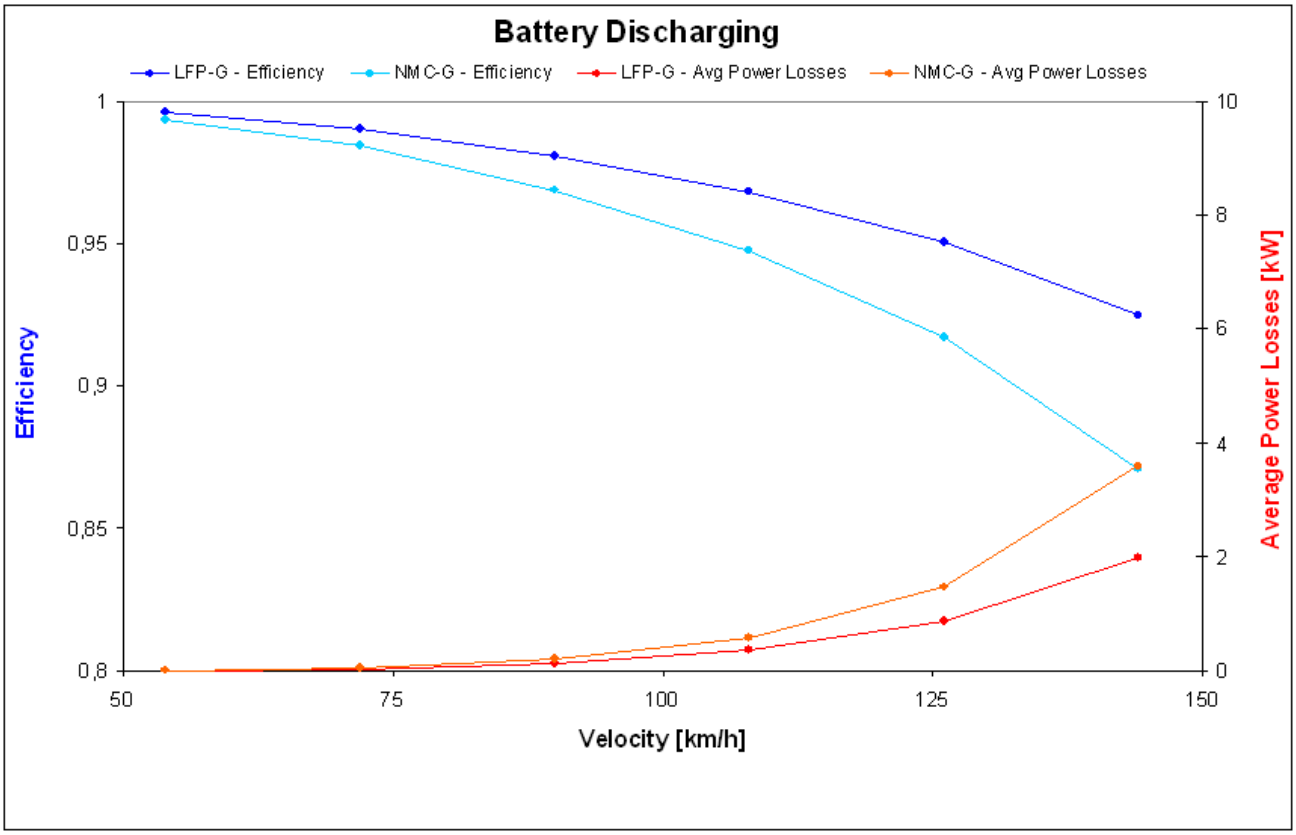

Figure 30: 16 kWh Battery, discharging efficiency and average battery power losses for different velocities

6.3.2 Driving Cycles

In order to analyze the battery behaviour in real driving conditions, vehicle simulation using different driving cycles is performed.
Driving cycles represent the speed of the vehicle over a period of time. They can be defined as *Static driving cycles*, and *Transient driving cycles*. In static driving cycles, such as the European NEDC, the set of data points is derived theoretically and in general include short periods of time where the speed is maintained constant. Transient driving cycles, such as the US FTP-75 are based on real life measurements taking in consideration to a representative driving pattern (Wikipedia).
Figure 31 shows the typical urban (FTP-75), and highway (FTP-HIGHWAY) US driving cycles together with the European NEDC (combination of urban and highway cycles).

Using these driving cycles simulation is performed and the traction and regeneration efficiency (due to regenerative braking in the deceleration phase) calculated for each considered cycle.
The vehicle considered has the typical characteristic of a mid-size vehicle present in the market today (mass m=1500 kg frontal area A_f= 2m^2, drag coefficient C_d=0.28, rolling friction coefficient C_r=0.01).

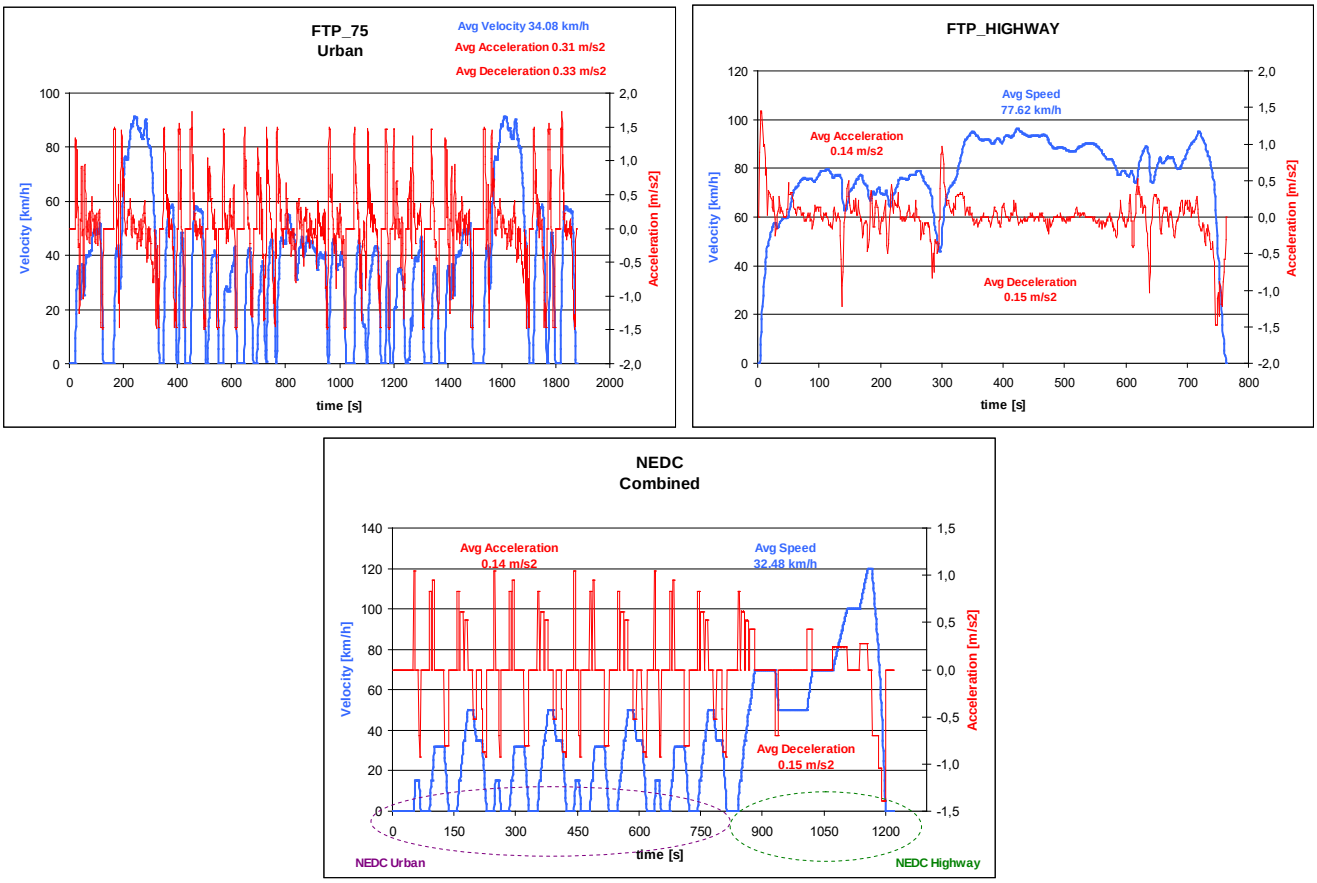

Figure 31: Speed (blue) and acceleration profile (red) for FTP-75, FTP-HIGHWAY and NEDC driving cycles

The energy provided by the battery, E_{trac}, and the energy losses, $E_{trac,loss}$, during the traction phase are calculated respectively integrating the battery power and the battery power loss (defined in 6.2.2) during the discharging phase when the battery is producing power for vehicle acceleration, $P_{BT} > 0$:

$$E_{trac} = \int_{t \in t_{trac}} P_{BT} dt \qquad \text{when } P_{BT} > 0$$

$$E_{trac,loss} = \int_{t \in t_{trac}} P_{loss} dt \qquad \text{when } P_{BT} > 0$$

The energies during the regeneration phase, when the battery is accumulating power due to the regenerative braking, $P_{BT} < 0$, are also calculated:

$$E_{regen} = \int_{t \in t_{regen}} P_{BT} dt \qquad \text{when } P_{BT} < 0$$

$$E_{regen,loss} = \int_{t \in t_{regen}} P_{loss} dt \qquad \text{when } P_{BT} < 0$$

The traction and regenerative efficiencies are calculated respectively as:

$$\eta_{trac} = \frac{E_{trac}}{E_{trac} + E_{trac,loss}}$$

$$\eta_{regen} = \frac{E_{regen}}{E_{regen} + E_{regen,loss}}$$

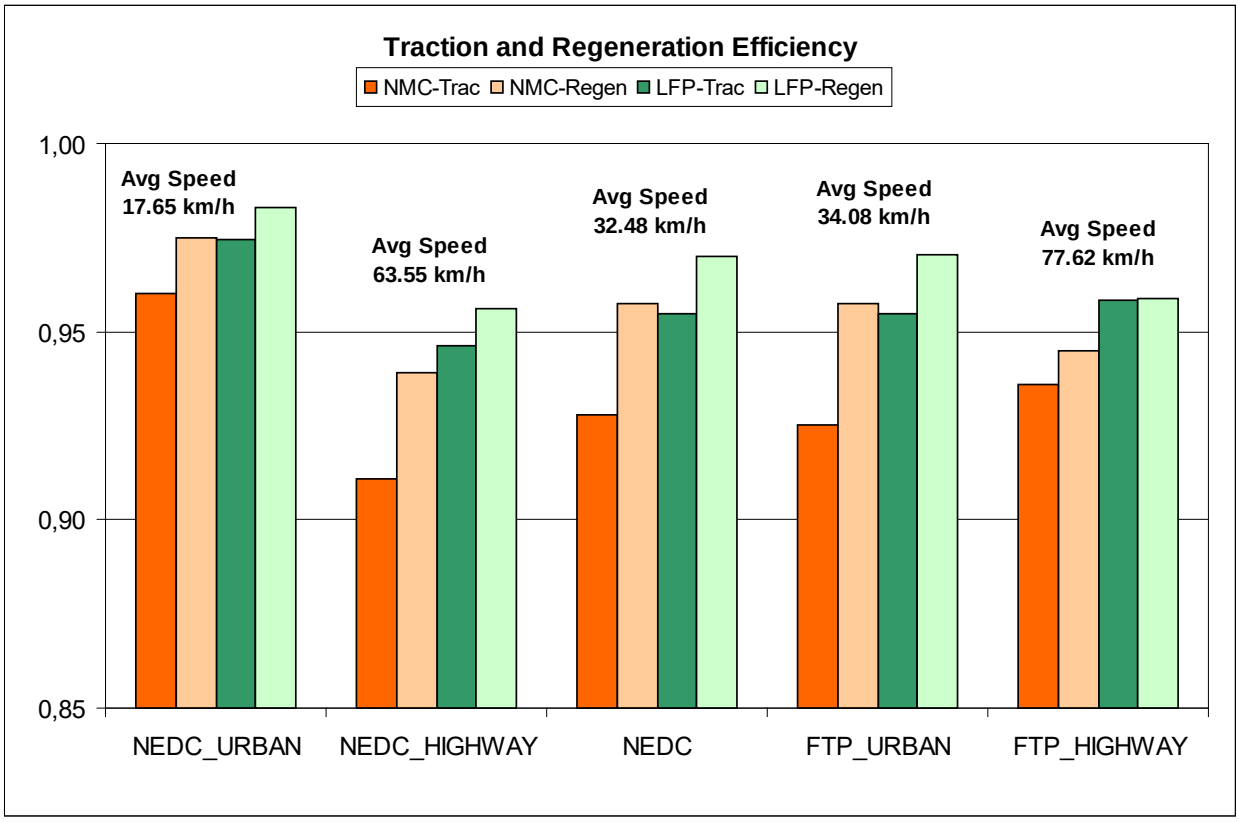

Figure 32: 16 kWh Battery - traction and regeneration efficiencies for different driving cycles

The results obtained show in general a lower efficiency, for both traction and regenerative phases for the NMC battery compared to the LFP. This is, once more, due to the higher internal resistance of this type of Lithium-Ion battery.
Due to the higher number of braking (and higher intensity), which a vehicle has to perform when driving in urban area, urban cycles such as FTP-75 and the urban part of the NEDC present a higher regenerative efficiency when compared to highway cycles.
Concerning the traction efficiency, the average cycle velocity plays a big role. High average vehicle speed lead to lower traction efficiency because more energy is lost due to the high and protracted current flow within the battery. The average velocity is not the only parameter that has to be considered in the evaluation of the traction efficiency. High accelerations have also influence on the traction efficiency.

7. Conclusion

In this work an integrated analysis of different Lithium-Ion battery types and their applications in the field of electric transportation has been given. An evaluation of the performance of different Lithium-Ion types used for EV applications taking into consideration various driving, charging and ambient temperature conditions was the main scope of this thesis.
The main parameters of the different chemistries have been assessed at cell and pack level in order to have a general and easy method to compare the performance that each type of battery may have under typical EV operating conditions.

Battery energy and power have been identified to be the two main parameters to define battery performance and they are strongly affected by the internal resistance, which depends on battery chemistry and operating conditions such as temperature, SOC and consumer usage. In order to assess these parameters battery and electric vehicle simulation models have been used.

First, a calculation of the internal resistance, specific energy and power, together with other parameters such as battery cost and weight for different Lithium-Ion chemistries for current and next generation electric cars has been performed, and a comparison between the various chemistries provided.
From this analysis we found that the NCA and the NMC graphite systems have the highest specific power and energy characteristics relative to other Lithium-Ion types, while the LMO and LFP cells have lower internal resistance and can thus provide high efficiencies in applications where high discharge/charge rates are requested. Even higher discharge and charge rates may be provided by Lithium Titanate cell (LMO-LTO). This chemistry presents the lowest internal resistance among all the Lithium-Ion battery types due to the absence of the SEI layer formation at the anode-electrolyte interface, however it suffers from low specific energy.

Since the internal resistance is essentially a representation of electrochemical reactions and transport processes inside the battery, it is strongly affected by the temperature and the state of charge of the battery. The effects of these parameters on the internal resistance have been also evaluated.
At high temperature the battery electrochemical kinetic is accelerated. The direct consequence of these effects is a lower internal resistance (and higher power capability) unfortunately associated to a drastically reduction of the battery lifetime. At low temperatures the opposite holds. If maintained at low temperatures, the battery can achieve higher lifetime but it suffers from an increase of the internal resistance and a loss of power.

These temperature effects together with the effects of a constant discharging/charging rate on energy and power capability have been further analyzed using an equivalent circuit model implemented in Simulink and Simscape for two different battery cells with different characteristics: NMC and LFP.
We found that the usable energy for both chemistries is dependent on the C-rate and on temperature. Temperature dependence starts to be not negligible at twenty degrees and strongly increases as the temperature gets lower and lower.
Considering the same temperature range the higher internal resistance values of the NMC results, at high C-rates, in a higher energy drop for this type of battery.

Finally with the NMC and LFP batteries implementation into a vehicle model typical charging/driving conditions and how they can affect battery efficiencies have been assessed.
Different charging powers, velocities and driving cycles have been used in order to evaluate the charging, discharging, as well as traction and regenerative efficiencies. We found that low internal resistance batteries, such as LFP, better react to fast charging conditions and high vehicle speeds. Furthermore they are also more efficient in urban driving conditions where many, and more intense, braking and accelerations are performed.

7.1 Future Work

Lithium-Ion technology is a quite new technology and much is still unknown about its behaviour, especially under real life applications of battery pack like the ones used for EV applications.
Nowadays many researchers are working on these topics and a lot of improvements have been achieved in recent times, however a lot of work is still required both at experimental and modeling level.

One big challenge that should be better analyzed is the effect of the degradation on the internal battery resistance growth with increasing storage and cycling time. This degradation effect has not been considered in this thesis and is very important in order to have a good battery performance prediction both at cell and pack level.
Battery performances, such as energy and power capability as well as lifetime, are also greatly influenced by the thermal behaviour of the cell and its heating influence of neighbouring cells. In this work this effect has not been assessed but thermal modeling, especially at pack level, can strongly improve the accuracy of performance evaluation.
In addition, a further consideration should be pointed out. In order to have a confirmation of the theoretical considerations presented in this thesis, they should be compared with experimental measurements that have not been possible to carry out during this work.

References

A. Burke, M. M. (2012). Fast charging tests (up to 6C) of lithium titanate cells and modules: electrical and thermal response. EVS26 International Battery, Hybrid and Fuel Cell Electric Vehicle Symposium. *Los Angeles, CA: EVS.*

Abuelsamid, S. (2010, July 15). More details on the construction and production of the Volt battery. *Retrieved November 26, 2012 from Autobloggreen: http://green.autoblog.com/*

AESC. (2007). AESC Products. *Retrieved October 30, 2012 from Automotive Energy Supply Corporation: http://www.eco-aesc-lb.com/en/*

Anegawa, T. (2009). Development of quick charging system for electric vehicles. *Technical Report, Tokyo Electric Power Company.*

B.Y. Liaw, E. P. (2003). Correlation of arrhenius behaviors in power and capacity fades with cell impedance and heat generation in cylindrical lithium ion cells. Journal of Power Sources , 119-121, *874-886.*

Battery University. (2012). Types of Lithium-ion. *Retrieved November 14, 2012 from Battery University: http://batteryuniversity.com*

BCG. (2010). Batteries for electric cars: challenges, opportunities, ant the outlook to 2020. *Boston Consulting Group. BCG.*

Blanco, S. (2010). Details on Nissan Leaf battery pack, including how recharging speed affects battery life. *Retrieved November 5, 2012 from Autobloggreen: http://green.autoblog.com/*

BP. (2012). BP statistical review of world energy June 2012. *BP. BP.*

Broussely, M. (2010). Battery requirements for HEVs, PHEVs and EVs: an overview. In G. Pistoia, Electric and Hybrid Vehicles: Power Sources, Models, Sustainability, Infrastructure and the Market. *Elsevier.*

Bullis, K. (2012, September 24). Will fast charging make electric vehicles practical? *Retrieved November 22, 2012 from MIT Technology Review: http://www.technologyreview.com*

CHAdeMO. (2010). What is "CHAdeMO"? *Retrieved November 22, 2012 from Coffee & Charge - CHAdeMO: http://chademo.com/*

D. Choi, W. W. (2011). Material challenges and perspectives. In H. L. X. Yuan, Lithium ion batteries: advanced materials and technologies. *Boca Raton, FL, USA: CRC.*

Eriksson, T. (2001). LiMn2O4 as a Li-Ion battery cathode. From bulk to electrolyte interface. *Acta Universitatis Upsaliensis, Faculty of Science and Technology, Uppsala.*

F.R. Kalhammer, H. K. (2009). Plug-in hybrid electric vehicles: promise, issues and prospects. EVS24 International Battery, Hybrid and Fuel Cell Electric Vehicle Symposium. *Stavanger, Norway: EVS24.*

FCVT. (2007). Plug-in hybrid electric vehicle R&D plan. *Plan, DOE - US Department of Energy, Energy Efficiency and Renewable Energy.*

Groll, M. (2012). Privates und offentliches laden. *eCarTec Congress Presentation, RWE Effizienz GmbH, Munich.*

H.G. Schweiger, O. O. (2010). Comparison of several methods for determining the internal resistance of lithium ion cells. Sensors , 10, *5604-5625.*

H.S. Choi, C. P. (2010, April 1). Towards high performance anodes with fast charge/discharge rate for LIB based electrical vehicles, lithium-ion batteries. *Retrieved November 28, 2012 from InTech: http://www.intechopen.com/*

Hofer, J. (2012). Modeling of electric vehicle energy consumption. *Presentation, Paul Scherrer Institut, Laboratory of Energy Systems Analysis, Villigen, Switzerland.*

Husain, I. (2011). Electric and hybrid vehicles: design fundamentals - 2nd Edition. *Boca Raton, FL, USA: CRC Press.*

IDL. (2008). Battery test manual for plug-in hybrid electric vehicles. *Idaho National Laboratory. Idaho Falls: IDL.*

IEA. (2012). Key world energy statistics. *International Energy Agency. IEA.*

IEA. (2012). Technology roadmap - Fuel economy of road vehicles. *International Energy Agency. IEA.*

IEC. (2001). Electric vehicle conductive charging system - Part 1: General requirements. *IEC.*

J. Vetter, P. N.-C.-M. (2005). Ageing mechanisms in lithium-ion batteries. Journal od Power Sources , 147, *269-281.*

J.B. Goodenough, Y. K. (2010). Challenges for rechargeable Li batteries. Chemistry of Materials , 22, *587-603.*

J.C. Hall, T. L. (2006). Decay processes and life predictions for lithium ion satellite cells. *Boeing - Saft Batteries, Satellite Development Center. AIAA.*

J.M. Tarascon, M. A. (2001). Issues and challenges facing rechargeable lithium batteries. Nature , 414, *359-367.*

K. Smith, M. E. (2012). Comparison of plug-in hybrid electric vehicle battery life across geographies and drive cycles. SAE World Congress and Exhibition. *Detroit, MI.*

K.G. Gallagher, P. N. (2011). Simplified calculation of the area specific impedance for battery design. Journal of Power Sources , 196, *2289-2297.*

Kohler, U. (2009). Hybrid electric vehicles: batteries. In P. Z. C.K. Dyer, Encyclopedia of electrochemical power sources *(1st ed., pp. 269-285). Elsevier.*

L. Guzzella, A. A. (2005). The QSS toolbox manual. *Manual, ETH Zurich, IMRT Measurement and Control Laboratory.*

L. Guzzella, A. S. (2007). Vehicle propulsion systems: introduction to modeling and optimization - 2nd edition. *Springer-Verlag.*

Lam, L. (2011). A practical circuit-based model for state of health estimation of Li-Ion battery cells in electric vehicles - MSc Thesis. *Delft: Delft University of Technology.*

Linden, D. (2002). Basic concepts. In T. R. D. Linden, Handbook of Batteries - 3rd Edition. *McGraw-Hill.*

M. Chen, G. R.-M. (2006). Accurate electrical battery model capable of predicting runtime and I-V performance. IEEE Transaction on Energy Conversion , 21 *(2), 504-511.*

M. Ecker, J. G. (2012). Development of a lifetime prediction model for lithium ion batteries based on extended accelerated aging test data. Journal of Power Source , 215, *248-257.*

M. Einhorn, F. C. (2013). Comparison, selection, and parametrization of electrical battery models for automotive applications. IEEE Transaction on Power Electronics , 28 *(3), 1429-1437.*

M. Tran, D. B. (2012, May). Realizing the electric-vehicle revolution. Nature Climate Change .

M. Wohlfahrt-Mehrens, P. A. (2009). Electrochemical energy storage systems for car applications. HySA Systems Business Seminar. *Cape Town, SA.*

M.Q. Synder, W. D. (2007). An infrared study of the surface chemistry of lithium titanate spinel (Li4Ti5O12). Applied Surface Science , 253, *9336-9341.*

Millner, A. (2010). Modeling lithium ion battery degradation in electric vehicles. IEEE Conf. CITRES, *(pp. 349-356).*

Novak, P. Storage in advanced batteries. *Presentation, Paul Scherrer Institute, Electrochemistry Laboratory, Villigen, Switzerland.*

P.A. Nelson, K. A. Advanced Lithium-Ion Batteries for Plug-in Hybrid-Electric Vehicles. *Argonne National Laboratory - EnerDel Corp.*

P.A. Nelson, K. G. (2011). Modeling of the performance and cost of lithium-ion batteries for electric-drive vehicles. *Argonne National Laboratory, Chemical Sciences and Engineering Division. ANL.*

P.C. Symons, P. B. (2002). Advanced batteries for electric vehicles and emerging applications: introduction. In T. R. D. Linden, Handbook of batteries - 3rd Edition. *McGraw-Hill.*

P.V. Braun, H. Z. (2011). Three-dimensional bicontinuous ultrafast-charge and -discharge bulk battery electrodes. nature nanotechnology , 6, *277-281.*

Pesaran, A. (2010). Current and future needs in electric drive vehicle batteries. Proc. of the 14th International Heat Transfer Conference. *Washington DC: ASME.*

S.S. Zhang, K. X. (2003). The low temperature performance of Li-Ion batteries. Journal of Power Sources *(115), 137-140.*

Saft Batteries. (2005). High-energy Saft VL45E datasheet. *Datasheet, Saft Batteries.*

Spotnitz, R. (2003). Simulation in capacity fade in lithium ion batteries. Journal of Power Sources , 113, *72-80.*

Srinivasan, V. (2008). Batteries for vehicular applications. American Institute of Physics Conference Proceedings *(pp. 283-296). USA: AIP.*

T. Christen, M. W. (2000). Theory of ragone plots. Journal of Power Sources *(91), 210-216.*

T. Huria, M. C. (2012). High fidelity electrical model with thermal dependence for characterization and simulation of high power lithium battery cells. IEEE .

T. Markel, A. B. (2002). ADVISOR: a system analysis tool for advanced vehicle modeling. Journal of Power Sources , 110, *255-266.*

Tahil, W. (2010). How much lithium does a Li-Ion EV battery really need? *Meridian International Research. Meridian International Research.*

Tang, M. (2010). Berkeley University Lectures - Battery Technology and Markets. *Lecture, Berkeley University, Battery Technology and Markets, Berkeley, CA.*

W. Zittel, J. S. (2007). Crude oil - the supply outlook. *Energy Watch Group.*

Wikipedia. (n.d.). Driving cycle. *Retrieved November 30, 2012 from Wikipedia: http://en.wikipedia.org/wiki/Driving_cycle*

Zhurkov, S. (1984). Kinetic concept of the strength of solids. Int. J. Fracture , 26, *295-307.*